Research in Computing Science

Volume 151(2)

ISSN: in process

Table of Contents

Salt and Pepper Noise Estimation in a Digital Image Using Convolutional Neural Network

Carlos Guerrero-Mendez[1], Tonatiuh Saucedo Anaya[1],
Daniela Lopez-Betancur[2]

[1] Universidad Autónoma de Zacatecas,
Unidad Académica de Ciencia y Tecnología de la Luz y la Materia,
Mexico

[2] Universidad Politécnica de Aguascalientes,
Dirección de Posgrado e Investigación,
México

guerrero_mendez@uaz.edu.mx, tsaucedo@uaz.edu.mx,
daniela.betancur@upa.edu.mx

Abstract. In this research work, a new technique for estimating impulsive, or salt and pepper noise in digital images is proposed. The estimation of the noise level in an image will serve as a diagnostic, and then facilitate actions to reconstruct an image with salt and pepper noise in digital image processing (i.e., using a filter of correct size). The technique estimates the noise factor in an image using the output of a convolutional neural network (CNN) and a multidimensional linear regression (MLR). The CNN is able to classify the noise factor and provides an output vector, and the MLR is able to use the output vector to estimate the level of noise in the images. For this study, different groups of random images were created with specific noise levels to train the CNN and to fit the MLR. A second dataset with intermediate noise values was used to evaluate the performance of the proposed technique. The proposed method achieves a repeatability of 0.87 and a mean error of 0.71 in salt and pepper noise values in the new images.

Keywords: Estimation of impulsive noise, salt and pepper, convolutional neural network.

1 Introduction

Digital images are prone to degradations and aberrations due to the occurrence of impulsive noise, also called "salt and pepper". This type of noise is visualized as random variations in intensity levels in a digital image and appears in the process of sending and receiving information. The causes of noise in an image (in real world) can be due to a malfunction or any damage (existence of dead pixels) in the image sensor or failures in the acquisition, hardware, and transmission [1]. Digital image processing techniques are useful as an easy and efficient way to deal with and remove unwanted noise or aberrations present in digital images. These techniques represent a digital

Table 1. Original images dataset. Image name: a) Cameraman, b) Eight, c) Trees, d) Moon, e) Coins, f) Lenna, g) Barbara, h) Mandrill, i) Honeybadger, j) Rice.
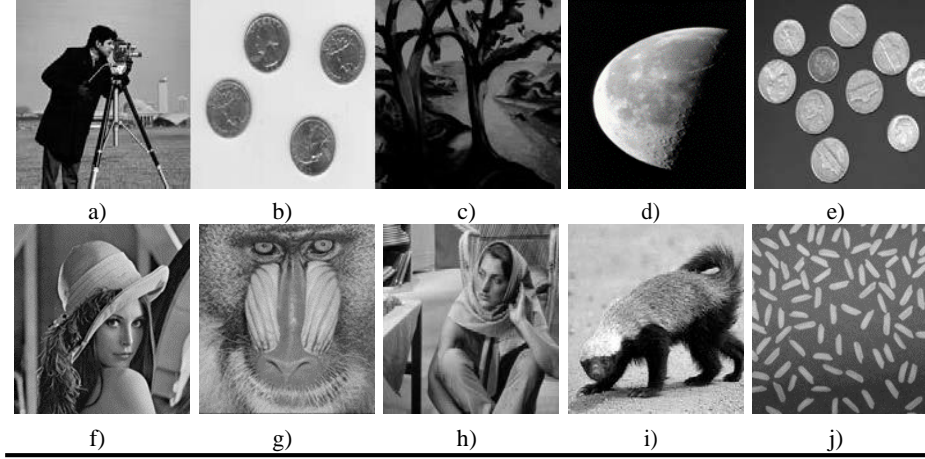
image as a matrix of numerical values and can operate mathematical transformations to treat digital images. There are many methods and techniques to remove impulsive noise in digital images, however, the most common resources to eliminate salt and pepper noise are the Median-type filters [2]

A promising new technology is convolutional neural networks, briefly called CNN. CNN tries to simulate the visual cortex in living beings, though using advanced operation blocks, and several layers of neurons [3]. Popularly, CNNs are used in object classification [4- 7] and detection [8- 11] tasks and semantic segmentation [12]. However, their versatility and power allow them to be implemented in an infinite number of applications [13- 16].

Since digital images can be expressed by numerical values and CNNs can decipher patterns within a large number of numerical values, then it is possible to find and estimate some value of interest within a pattern in an image. Previously, the use of a CNN and a multivariate linear regression (MLR) was introduced by Carlos Guerrero-Mendez et al [17] to estimate the phase difference between digital holograms. Therefore, this research is significant because by applying the correct median filter size to an image, we can reconstruct it correctly and avoid processing an image using too large a median filter, which degrades or removes important information in the image.

2 Materials and Methods

This research report focuses mainly on: the generation of data, the training of a CNN using the transfer learning technique, the fitting of an MLR to approximate the noise value, and finally the evaluation of the results obtained.

Table 2. Sample images of each class from the training dataset using the "Moon" image.

0				
0.1	0.2	0.3	0.4	0.5
0.6	0.7	0.8	0.9	1
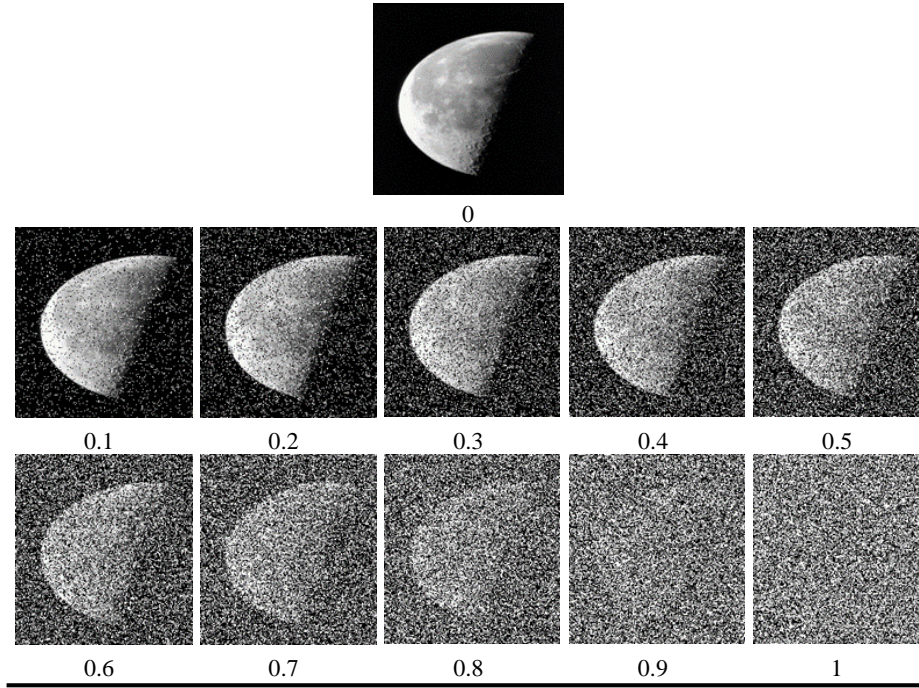
2.1 Image Generation

The training dataset was created from a common set of images used for image processing tasks. The set of seeds or sample images consists of 10 images that can be viewed in Table 1.

2.2 Training Dataset

In the training dataset, different noise factors of 0, 0.1, 0.2, 0.3, 0.4, 0.5, 0.6, 0.7, 0.8, 0.9 and 1 salt and pepper were inserted in each image in the seed set. Based on the values of the noise in the images, 11 categories or training classes were created to train the CNN architecture. In total, the training dataset consists of 11,000 images divided into 11 classes. Each class of the training dataset has 1,000 images, of which 100 images are generated using a single noise factor per image sample. Table 2 shows some examples of the training classes using the noise factors in the image "Moon".

2.3 Data Augmentation

Training a CNN architecture requires a large number of images and its labels, in the case of supervised learning. Generally, depending on the number of images in the training datasets a CNN architecture can learn and detect more patterns in an image. In addition, overfitting in the CNN model is avoided. The lack of images in the training dataset can be solved using the "data augmentation" technique, which creates new images only for the training process based on some random digital transformations [18]. As part of this research, new images were created using the flipped horizontal transformation.

2.4 Validation Dataset

Once the CCN has been trained, the performance for the classification task is validated. In the validation step, similar or new images of the same classes are implemented in the training process to assess the learning of the model. In this research, 250 images were generated for each class of salt and pepper noise factor for the validation dataset. The 10 sample images were used in each class and we added 25 times the same noise factor in each image. So, the total number of images in the validation dataset is 2750.

2.5 CNN Architecture

The CNN model used in this research is called AlexNet, which has a simple CNN architecture and is easy to train. The AlexNet model has 60 million parameters and 650,000 neurons. The feature extraction process is done using five convolutional layers, while the classifier process uses three fully-connected layers. AlexNet uses a ReLU. Nonlinearity activation function that allows the training process to be performed much faster than using the activation functions of Tanh and Sigmoid [19]. The output of a CNN is an array of numbers that represent the probabilities that the CNN will assign the input data to an output category. There are probabilities raw values between $-\infty$ to $+\infty$ of the input data, called Logits, which can be obtained from the last layer of the CNN before the Softmax layer.

2.6 Transfer Learning

Training a neural network from random initial values (weights and bias) is a task that requires a large amount of computational resources and training time. Furthermore, to consider the performance of a neural network as acceptable, it must be trained with a large number of labeled images. There are large databases of labeled images that are used to train neural networks architectures; these databases are usually composed of a large number of common objects, as in ImageNet [20]. When a neural network is trained to classify images in some task, it is possible to use this knowledge acquired by the neural network to classify other types of images in another task, i.e., we use the weights and biases of a neural network to classify a task, and from this acquired knowledge, adjust a second training, with new images, the weights, and biases for a
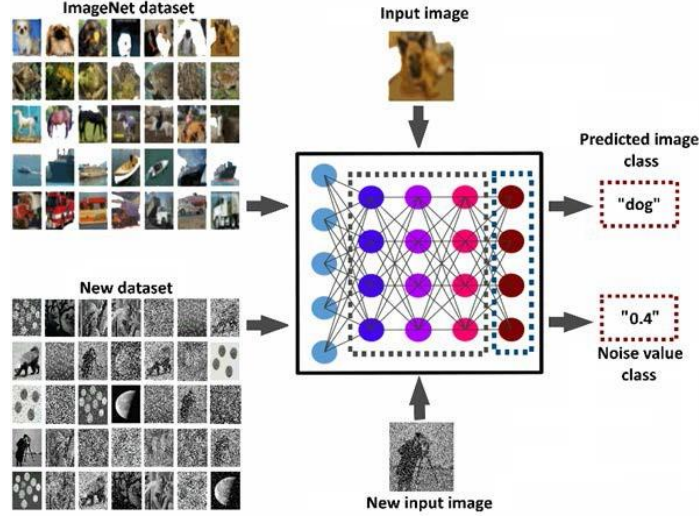
Fig. 1. Transfer learning using new images.
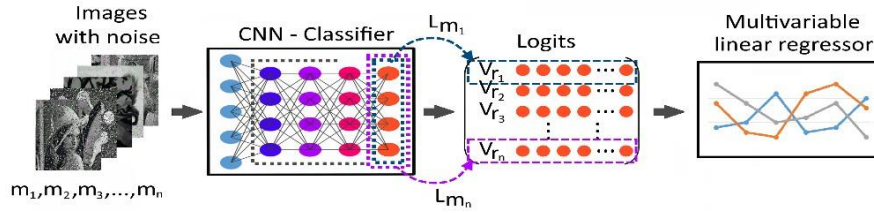
Fig. 2. Diagram of creation of a Logits dataset to fit an MLR.

new classification. In this paper, the AlexNet CNN model, trained with ImageNet, was implemented using transfer learning to classify the noise images (see Fig. 1).

Once the classifier has been trained, the next step is to create a database using the Logits vector extracted from the last layer of the CNN (before the Softmax function) using each image of the training dataset. The new database will contain the logits that will be used to fit the MLR. Fig. 2 shows a diagram of the creation of a dataset with the logits of the images.

The proposed technique uses an algorithm in which we enter an image with an unknown noise value, later, the value of the noise factor in the image will be given as an output. That is, the algorithm receives an image with noise as input, then the image is processed by the CCN, and the Logits vector passes to the MLR as input, and finally, we get the noise factor in the image. This entire process is illustrated in Fig. 3.
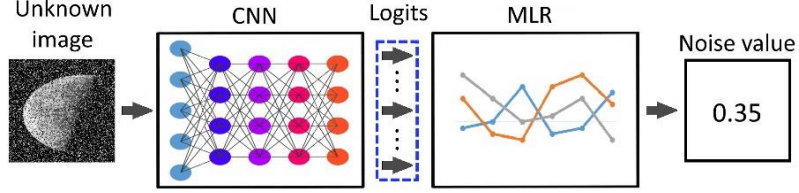
Fig. 3. Noise estimation in an unknown image.

2.7 CNN and MLR Performance Metrics.

One of the most used tools to evaluate the training performance of a CCN is the confusion matrix. Using the confusion matrix, we can graphically observe the results of classifying the images in the validation dataset. In addition, we can also observe where our classifier has classification problems, and change the training options to obtain better results. By implementing the confusion matrix, we can extract some basic parameters or data, and using them we can develop metrics more powerful. The basic parameters are: The true positive (TP) which are the number of predicted cases that belong to a class and that were correctly classified to belong to a class. False positive (FP) are the number of predicted cases that belong to a class, but they really do not belong to the class. True negative (TN) refers to the predicted cases that do not belong to a class and they do not belong to the class. and False Negative (FN) which are the elements classified that do not belong to a class but they really belong to a class. Using TP, FP, TN and FP we can develop the metrics of: accuracy, precision, recall, specificity, f-score. For evaluation of the MLR, the metrics were used: Coefficient of determination (R2), mean absolute error (MAE), mean square error (MSE) [17].

3 Experimental Results

3.1 Salience Maps

A useful tool to analyze the learned features during the training process is the saliency maps [21]. By analyzing the salience maps of a CNN, we can observe which regions of an image provide a greater degree of activation in the artificial neurons of a CNN model. In other words, a Salience map shows the areas in an image in which a CNN concentrates to perform a classification.

Although the predicted class is not the main interest in this research, it is important to analyze what the CCN classifier defines as important and to understand some of the patterns found in the image to be classified. When analyzing the image samples (clean images), we observe that there is a pattern of activations in the areas where the silhouettes are defined. In Table 3 we can view the activation regions in original images.

Table 3. Salience maps of "Cameraman" images with a noise level of 0.0.
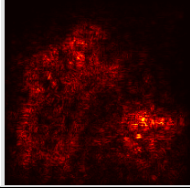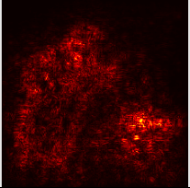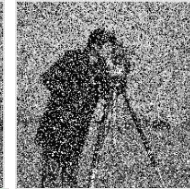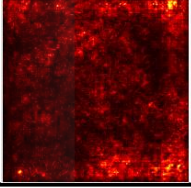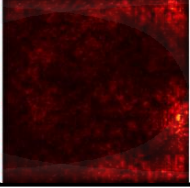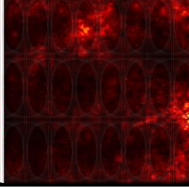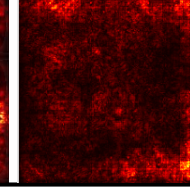
Table 4. Salience maps of "Cameraman" images with a noise level of 0.4.

However, if you want to classify the same image where only the noise factor was added (see Table 4), the CNN will not be able to find a single or similar pattern, and it won't even try to find the patterns found in the clean image, but it bases its classification on the use of patterns generated by pixel variations caused by noise in the image.

3.2 CNN Training Process

The training process algorithm was executed using the free Google Colab cloud service, which is a research tool for machine learning education and research. Colab allows us to write and execute Python code through a Jupyter notebook environment that runs on servers of Google. One of the great qualities of this cloud service is that we use for 12 hours a virtual machine that has specialized hardware such as a graphics processing unit (GPU). A GPU improves computing performance like matrix multiplication, which is a common and time-consuming computation operation in Deep Learning [22]. In this research, the CNN training was performed on a Tesla T4 GPU,

8

Table 5. Hyperparameters used in the training process.

Hyperparameter	Value
Optimization algorithm	Mini-batch gradient descent
Epochs	100
Learning rate	0.001
Batch size	32
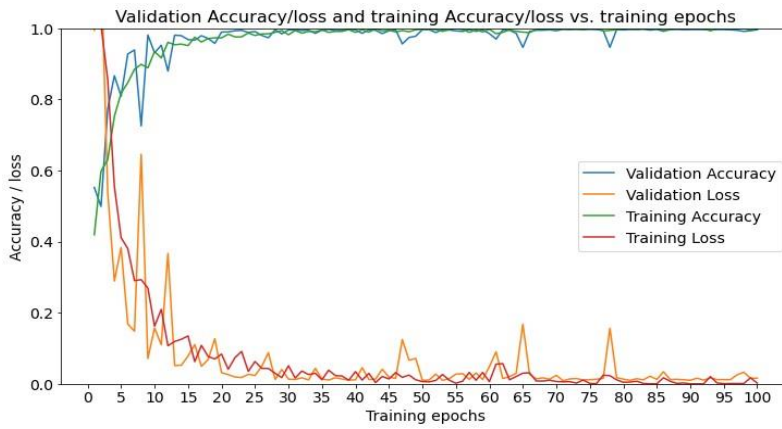
Fig. 4. Accuracy/loss evolution in the training process.

also, the Python code was developed using the Pytorch 1.9.0+cu102 library. The CNN model and other tools necessary for CCN training were obtained from Torchvision 0.10.0+cu102. According to the training parameters, we used the Gradient descent as the optimization algorithm and the loss was calculated using CrossEntropyLoss, a total of 100 training epochs were implemented, with a batch size of 32 and a learning rate of 0.001. Table 5 lists the main

Hyperparameters implemented.

According to the evolution and behavior of the accuracy and loss values, indications of overfitting in the training process are discarded (see Fig 4).

On the other hand, we observe that the confusion matrix has high accuracy to predict the true classes in the training images (see Fig 5).

The CCN training process was evaluated using the validation dataset with the metrics of accuracy, precision, recall, specificity. Using 100 training epochs, it was found that the best training epoch according to its accuracy and loss was epoch 91. Table 6 lists the validation metrics in the training process at epoch 91.
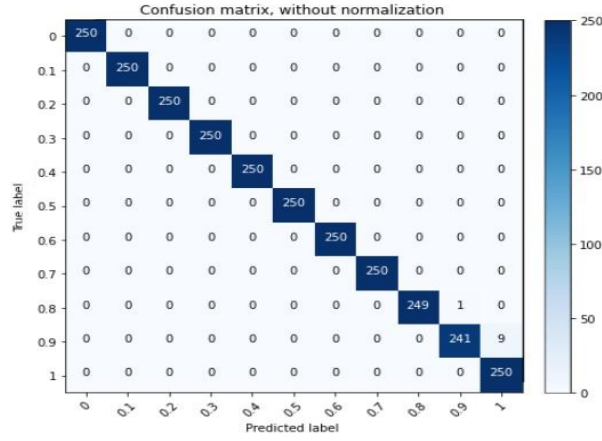
Fig. 5. Confusion matrix obtained in the training process.

Table 6. CNN training validation metrics.

Metric	Value
Accuracy	0.9967
Precision	0.9968
Recall	0.9967
Specificity	0.9997
Training time	116m 50s

3.3 Validation of the Noise Estimation Technique

Training a CNN to classify images based on their noise value is a trivial task that does not require much complexity. The use of the training and validation datasets to validate the estimation process may not be entirely appropriate. Using an MLR would make it possible to predict the magnitude of the intermediate noise value in a new image. To validate the operation of the proposed method, classes with intermediate values were created to estimate and compare the noise value in the image The noise factor values for the intermediate images are: 0.05, 0.15, 0.25, 0.35, 0.45, 0.55, 0.65, 0.75, 0.85, 0.95.

As a result, 1,000 images were created to validate the proposed technique. Table 7 shows some examples of the different noise intermediate values applied in the "Cameraman" sample image.

Table 7. "Cameraman" with intermediate noise values.

| 0.05 | 0.15 | 0.25 | 0.35 | 0.45 |

| 0.55 | 0.65 | 0.75 | 0.85 | 0.95 |
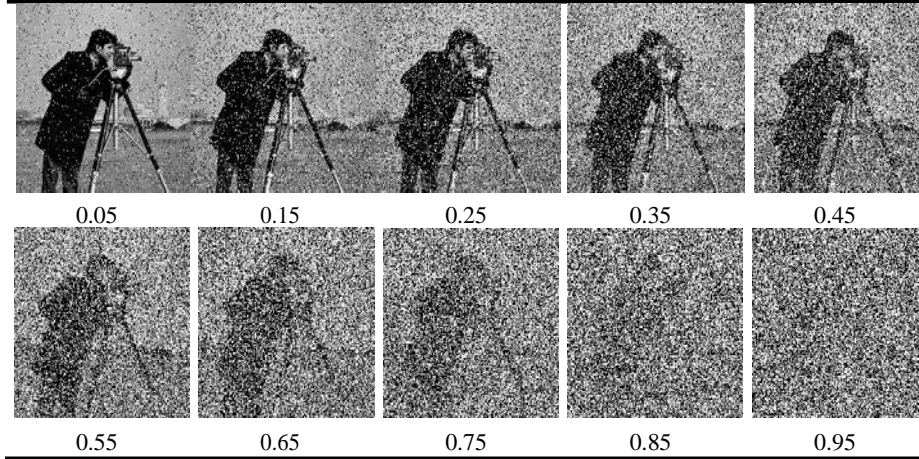
Table 8. MLR performance metrics.

Metric	Value
R^2	0.8703
MAE	0.0716
MSE	0.0106
Standard deviation	0.2631

The values of the performance reached by the proposed technique are shown in Table 8. The values reached demonstrate excellent behavior, and a good repeatability. This indicate that the CNN could be used as technique for image denoising process without the need to implement arduous digital image processing techniques.

4　Conclusions

In this article, a novel method for estimating salt and pepper noise in digital images was presented. The noise value is performed using a CNN and a regression model. This method can be the first step in implementing an image denoising process. Given that, knowing the correct amount of noise, an accurate image filter can be applied. According to the results obtained, a CNN can focus on the number and distribution of black and white pixels in an image. In addition, we have demonstrated that the output of a CNN can be used to link to other parameters or aspects of interest through an MLR. The results showed high accuracy in the estimation of salt and pepper noise added to an image, even in images with a noise factor with which the CNN was not trained. As future work, a complete analysis of the use of different CNN models will be developed. In addition, different regression models will be tested and the dropout process will be

analyzed using different values. Furthermore, an analysis is required for the implementation of median filters for an optimal size according to the noise level of the salt and pepper in the input image.

References

1. Djurović, I.: BM3D Filter in Salt-and-Pepper Noise Removal. EURASIP Journal on Image and Video Processing, 13 (2016) doi: 10.1186/s13640-016-0113-x.
2. Liang, H., Li, N., Zhao, S.: Salt and Pepper Noise Removal Method Based on a Detail-Aware Filter. Symmetry, 13, pp. 515 (2021) doi: 10.3390/sym13030515.
3. Qin, Z., Yu, F., Liu, C.: How Convolutional Neural Network See the World-A Survey of Convolutional Neural Network Visualization Methods, arXiv (2018) doi: 10.48550/arXiv.1804.11191.
4. Khan, A., Sohail, A., Zahoora, U.: A Survey of the Recent Architectures of Deep Convolutional Neural Networks. Artificial Intelligence Review, 53, pp. 5455–5516 (2020) doi: 10.1007/s10462-020-09825-6.
5. Lopez-Betancur, D., Bosco Duran, R., Guerrero-Mendez, C.: Comparación de arquitecturas de redes neuronales convolucionales para el diagnóstico de COVID-19. Computación y Sistemas, 25 (2021) doi: 10.13053/cys-25-3-3453.
6. Ortiz-Preciado, A.A., Vega-Fernández, J.A., Ochoa-Ruiz, G.: Clasificación de enfermedades del tórax usando aprendizaje profundo y aumento de datos de calidad en el conjunto de datos ChestX-ray8. RCS, 148, pp. 41–53 (2019) doi: 10.13053/rcs-148-8-3.
7. Colmenares Guillen, L.E., Torres López, R.G., Carrillo Ruiz, M.: Clasificador de edad en imágenes digitales usando métodos estadísticos. RCS. 140, pp. 91–104 (2017) doi: 10.13053/rcs-140-1-8.
8. Liu, L., Ouyang, W., Wang, X.: Deep Learning for Generic Object Detection: A Survey. International Journal of Computer Vision. 128, pp. 261–318 (2020) doi: 10.1007/s11263-019-01247-4.
9. Zou, Z., Shi, Z., Guo, Y..: Object Detection in 20 years: A Survey, arXiv (2019) doi: 10.48550/arXiv.1905.05055
10. González Frayre, G.F., Olvera Olvera, C.A., López Monteagudo, F.E.: Estudio y comparativa de algoritmos de detección de objetos con redes neuronales artificiales convolucionales para la detección de enfermedades en hojas, Universidad Autónoma de Zacatecas (2019) doi: 10.48779/p41k-fx69.
11. Takieddine Seddik, M., Kadri, O., Bouarouguene, C.: Detection of Flooding Attack on OBS Network Using ant Colony Optimization and Machine Learning, Computación y Sistemas, 25 (2021) doi: 10.13053/cys-25-2-3939.
12. Garcia-Garcia, A., Orts-Escolano, S., Oprea, S.: A Survey on Deep Learning Techniques for Image and Video Semantic Segmentation. Applied Soft Computing, 70, pp. 41–65 (2018) doi: 10.1016/j.asoc.2018.05.018.
13. Mamoshina, P., Vieira, A., Putin, E.: Applications of Deep Learning in Biomedicine. Molecular Pharmaceutics, 13, pp. 1445–1454 (2016) doi: 10.1021/acs.molpharmaceut.5b00982.

12

14. Luong, N.C., Hoang, D.T., Gong, S.: Applications of Deep Reinforcement Learning in Communications and Networking: A Survey, IEEE Communications Surveys & Tutorials, 21, pp. 3133–3174 (2019) doi: 10.1109/COMST.2019.2916583.

15. Zhao, R., Yan, R., Chen, Z.: Deep Learning and its Applications to Machine Health Monitoring. Mechanical Systems and Signal Processing, 115, pp. 213–237 (2019) doi: 10.1016/j.ymssp.2018.05.050.

16. Ortiz-Rodriguez, J.M., Guerrero-Mendez, C., Martinez-Blanco, M. del R.: Breast Cancer Detection by Means of Artificial Neural Networks. Advanced Applications for Artificial Neural Networks, pp. 161–179 (2018) doi: 10.5772/intechopen.71256.

17. Guerrero-Mendez, C., Saucedo-Anaya, T., Moreno, I.: Digital Holographic Interferometry without Phase Unwrapping by a Convolutional Neural Network for Concentration Measurements in Liquid Samples. Applied Sciences, 10, pp. 4974 (2020) doi: 10.3390/app10144974.

18. Wang, J., Perez, L.: The Effectiveness of Data Augmentation in Image Classification Using Deep Learning. Convolutional Neural Networks Vis. Recognit, 11, pp. 1–8 (2017) doi: 10.48550/arXiv.1712.04621.

19. Maeda-Gutierrez, V., Galvan-Tejada, C.E., Zanella-Calzada, L.A.: Comparison of Convolutional Neural Network Architectures for Classification of Tomato Plant Diseases. Applied Sciences, 10, pp. 1245 (2020) doi: 10.3390/app10041245.

20. Deng, J., Dong, W., Socher, R.: Imagenet: A Large-Scale Hierarchical Image Database. In: IEEE Conference on Computer Vision and Pattern Recognition, pp. 248–255 (2009) doi: 10.1109/CVPR.2009.5206848.

21. Parkhurst, D., Law, K., Niebur, E.: Modeling the Role of Salience in the Allocation of Overt Visual Attention. Vision research, 42, pp. 107–123 (2002) doi: 10.1016/s0042-6989(01)00250-4.

22. Huang, Z., Ma, N., Wang, S.: GPU Computing Performance Analysis on Matrix Multiplication. The Journal of Engineering. 2019, pp. 9043–9048 (2019) doi: 10.1049/joe.2018.9178.

Scope of Linear Genetic Programming in the Search for Kinematics Models for a 3 DOF SCARA Robot Subjected to Path Following

Humberto Velasco Arellano, Martín Montes Rivera

Universidad Politécnica de Aguascalientes,
Maestría en Ciencias en Ingeniería,
Mexico

mc160006@alumnos.upa.edu.mx, martin.montes@upa.edu.mx

Abstract. Robotic arms have played a significant role in industrial and technological development, automating several jobs efficiently. Its main task is the tracking of defined trajectories, for which it uses a model known as inverse kinematics. This work uses linear genetic programming to solve the trajectory tracking in robots of 3 degrees of freedom with the least amount of information possible. The efficiency is analyzed on the requested route and evaluating the resulting model on different paths. This work demonstrates the tendency to optimize the local minimum and how the results are only valid for the optimized route due to the lack of information about other possible points or trajectories.

Keywords: Linear Genetic programming, path following, automatic robot modeling, inverse kinematics.

1 Introduction

Robotics is the study and design of multifunctional manipulators, capable of moving materials, parts, tools, or special devices, according to variable trajectories, programmed to perform various tasks [1]. However, this branch of science has transcended throughout history, showing scientific and technological advances applied to multiple areas of knowledge [2].

The kinematics considers robots as input-output systems, where the articular variables or inputs are associated with the movement of each motor independently, and the output or Cartesian variables describe the position and orientation of the end effector [1].

Being of interest inverse kinematics (IK onwards), to know the position and orientation of the end effector, in this way, it is possible to see the status of each joint and its movement to follow a given path [3].
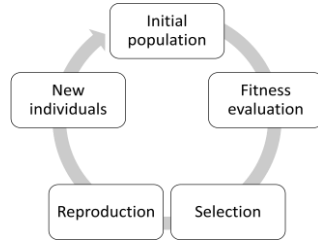
Fig. 1. GP operation in natural selection cycle [8].

There are deterministic methods to obtain the IK model that defines each robot; however, this process becomes complex with increasing degrees of freedom (DOF onwards) [4].

Machine learning allows solving high complexity problems automatically, being an alternative to solving the IK model. Genetic programming algorithms (GP onwards) are backward search algorithms that can solve problems under an unknown operation, also called black-box testing. However, GP only covers the structural search and not the content of the solution [5- 7].

The GP algorithm follows the natural selection cycle of evolutionary algorithms, as shown in Fig 1.

GP conventionally uses individuals defined as a tree structure. However, individuals of linear GP with equation structures produce a lower computational cost [8].

1.1 Related Works

In recent years the works that describe the IK model produced contributions using algebraic models for tool manipulation [9], a human arm description using the integral workspace [10], and even mimicry mechanisms for the path of the arms in an NAO robot [11].

On the other hand, computational science tries to solve using neural networks [12- 14] and genetic algorithms [15, 16].

Some works identify the arm trajectory of an NAO robot using IK [18], the IK model obtained with iterative methods [19, 20], as well as specialized controls in the upward approach of robotic arms using the Jacobian [21] and offline strategies [22].

These problems have been transferred to parallel robots [23], human-robot interaction interfaces [24] and movile robots [25].

The GP properties give a proposal to cover the problem described. This method reported [26] highlighted the benefits of this method. However, it was not until the works [17,27] that the proposed method was applied, finding an approach of the IK solution in 6 DOF robots.

2 Theoretical Framework

A robot manipulator composition includes joints and links; the links are the rigid structural elements, while the joints are the existing connections between links, which allow the relative movement between them; each joint adds DOF to the robot, depending on its morphology [1].

Kinematics is the science that analyzes these structures, in this case, called robots, and their movements in space independently of the force that generates them [4].

2.1 Inverse Kinematics

The inverse kinematics approach produces nonlinear and coupled equations for describing the three-dimensional motion in conjunction with orientation in a Cartesian space [2].

This procedure needs to obtain the homogeneous matrices describing each link under the Denavit-Hartenberg convention and thus obtain the inverses of these matrices [1].

These matrices premultiplied the transformation matrix described in (1):

$$T = \begin{bmatrix} n_x & o_x & a_x & p_x \\ n_y & o_y & a_y & p_y \\ n_z & o_z & a_z & p_z \\ 0 & 0 & 0 & 1 \end{bmatrix} \tag{1}$$

Applying the process in (2), are obtain a set of cleared equations for each joint:

$$(A_1{}^0)^{-1} * T = A_2{}^1 * \ldots A_n{}^{n-1} \tag{2}$$

Path following. Most robot applications require a proposed route, approaching the search of trajectories from different points of view [4].

One of the problems is the search for the optimal path [28]. Other works focus on the lower consumption of resources by the motors involving the dynamics of the robot [29] and the smooth path approach for specific applications [30].

2.2 Linear Genetic Programming

The GP is an evolutionary algorithm specialized in developing computer programs to solve given problems; this algorithm is a specialization of the genetic algorithms with the difference that the individuals used are complete programs [5, 31].

These algorithms are inspired by the adaptation of species and follow the cycle shown in Fig. 1.

The algorithm starts with initializing the population of individuals representing possible solutions; evaluation of the fitness. Then the tournament selection takes individuals better able to reproduce and inherit their genes, as illustrated in Fig. 2.
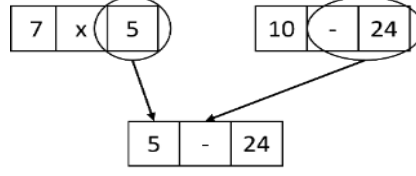
Fig. 2. Selection and crossover representation for GP algorithms [32].
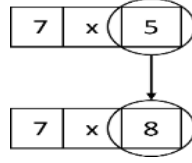
Fig. 3. Mutation representation for GP algorithms [32].

These processes increase the possibility of mutation, where one allele is randomly changed, using the Node Replacement Mutation [5, 33], shown in Fig. 3.

Furthermore, this process is repeated over a known number of generations or until the desired goal is reached [5].

3   Methodology

This section describes the experimental setup and the GP solution to find the model of a robotic arm following a known path and check whether the results obtained describe the IK or optimize a local minimum.

3.1 Design of Experiment

Start from the assumption that the purpose of a robotic arm must follow a path for a given task; the problem consists of knowing the kinematic model that describes the robot along with that movement.

It is considered an input-output system, where the expected coordinates of the end effector along the path are known as input and need to know the positions of each joint to achieve the task as output, restricting the movement between point and point to involve a slight change in the joints.

A linear GP algorithm builds its individuals using integers from 0 to 9, operators for addition, subtraction, multiplication and division operations, sine and cosine functions, and Cartesian coordinates, x, y, and z, as variables.

Was used a proposed 3 DOF SCARA morphology, with links of 200 mm in length each, because it is a robot with a known kinematic model and is typical morphology in electronic assembly lines.

Were set two different study cases; both paths move from end to end in the work area; the first route described in (3), with x1, y1, z1, contemplates a straight trajectory
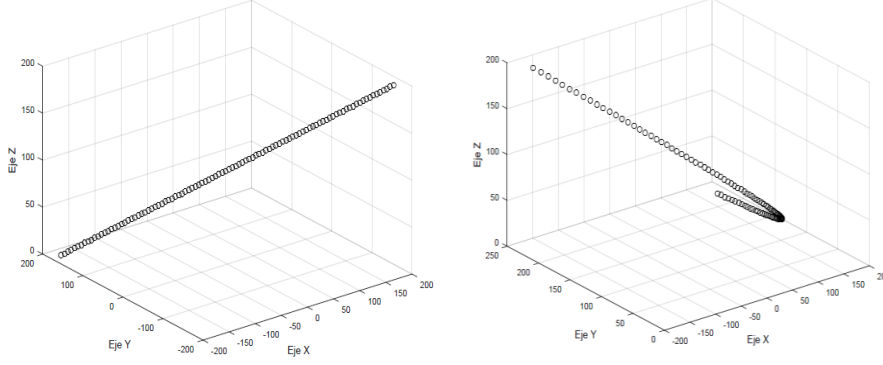
Fig. 4. a) The first case path follows; b) The second case path follows.
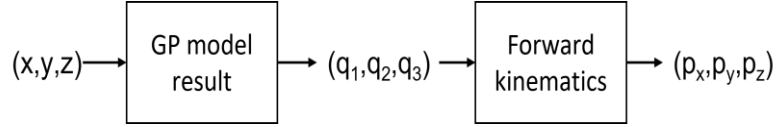
Fig. 5. Block diagram for GP objective function used.

shown in Fig. 4 a). The second case corresponds to a curved path in (3), with x2, y2, z2, and its trajectory corresponds to Fig. 4 b):

$$x1= [-180,180]; \qquad x2= [-180,180];$$
$$y1= [180, -180]; \qquad y2=(x/12)^2;$$
$$z1= [0,200]; \qquad z2= [200,0];$$

(3)

All tests were simulated in MATLAB 2015b using structured code without using special commands.

3.2 Objective Function

To evaluate the individual's fitness were separated into three equations, which represented the model of each joint; then, feeding the equations with the points of the trajectories mentioned above (x,y,z). Finally, the results obtained (q1, q2, q3), fed to the model in direct kinematics and checked if these results (px, py, pz) led to the requested path shown in Fig. 5.

The individual fitness was the absolute difference in millimeters between the requested point and the obtained position, as shown in (4):

$$Fitness=abs(x-p_x) + abs(y-p_y) + abs(z-p_z)$$

(4)

6
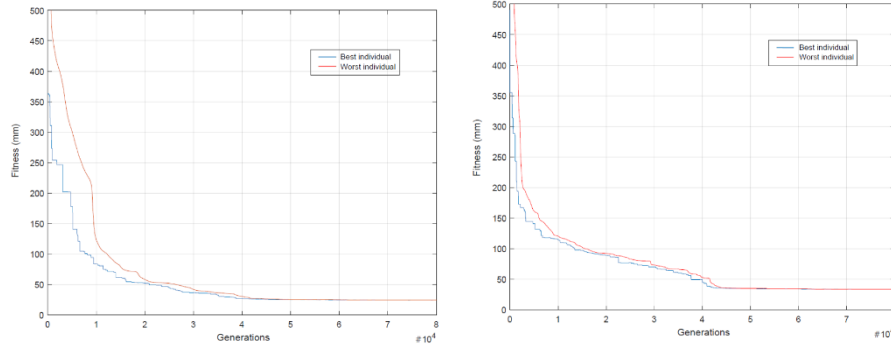
Fig. 6. a) Population adaptation in GP case 1, b) Population adaptation in GP case 2.

Table 1. Initial condition used in the GP algorithm.

Parameter	Value
Population size	2500
Generations	80000
Tournament size	3
Genes	6
Alleles	7
Mutations per generations	28
Seed	1

3.3 GP Algorithm

The selection of initial conditions was according to the rules described in the literature [5], maintaining the population diversity as many generations as possible. Table 1 shows the values.

The individuals contain three independent equations to describe the kinematics, and each equation is dependent on the three cartesian axes x,y, and z (5):

$$\text{Individual}(1,1) = f(x,y,z);$$

$$\text{Individual}(1,2) = f(x,y,z); \tag{5}$$

$$\text{Individual}(1,3) = f(x,y,z);$$

4 Results

According to the experiment, both cases give expected adaptation results, decreasing the error as the generations progress. Fig. 6 shows in blue the adaptation of the best
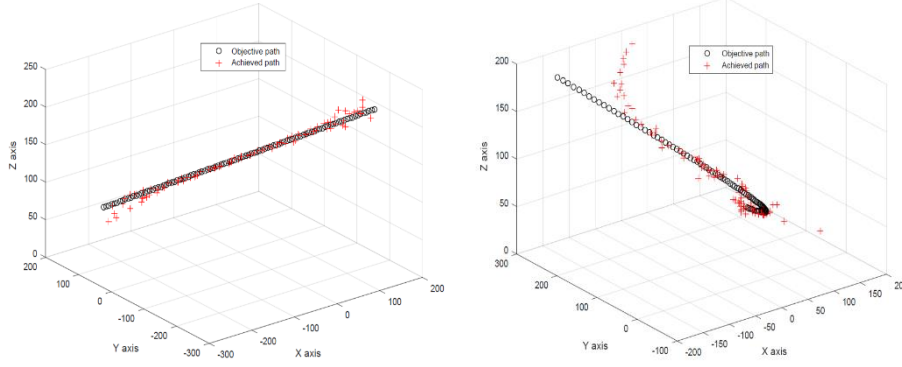
Fig. 7. a) GP model performance for case 1 path, b) GP model performance for case 2 path.

individual and how it decreases. On the other hand, the red line shows the worst individuals, representing the population diversity as the distance between these lines, disappearing at the end of the generations, being Fig. 6a) the linear path for the first case and Fig. 6b) the curve path on the second case.

As can be seen in case 1, with a linear path as the objective, the algorithm has an accelerated adaptation respect case 2, concluding that the complexity and variation in the objective path slow down the adaptation of the algorithm:

$$
\begin{cases}
q_1 = x + \sin(y) - z - 0.1821x - 0.5\cos(x)\cos(y) - \sin(y)^{\sin(x)} + 9 * 4^{\sin(y)} - (\sin(y)^2 - \sin(y)^{2.7183} + 10.8731)(\sin(y)^4 + \sin(y) + 0.0416z) + 40 \\[2mm]
q_2 = y + 1.414z + \dfrac{(3^x + \frac{1.812}{\cos(y)})(2.718z + \frac{9}{\cos(y)} + \frac{x\cos(x)}{\cos(z)})}{(0.399\sin(z) - y^4)(\frac{2.718}{y^5} - \cos(y) + 4)(2.718^x - 0.367\cos(y)^y + 1296)} + 3 \\[2mm]
q3 = z + 0.833y + \dfrac{z - \frac{3\cos(x)\sin(z)}{2.718^{\sin(x)}}}{x^{6z} - 262134} + \dfrac{y}{x} - \dfrac{1}{(\frac{2\sin(x)}{\sin(z)} + 6.2817)^{5z + \sin(x)}} - 49
\end{cases}
\tag{6}
$$

$$
\begin{cases}
q_1 = x + \dfrac{\sin(x)^6}{\cos(z)} - z - 0.333\cos(x) - \cos(z) - \dfrac{\frac{13.2436}{\cos(z)} - 2}{403.428\sin(y) + 5} - 0.75x + \dfrac{0.2333xz}{y} - 35.027 \\[2mm]
q_2 = y + 0.111z - 1.333y - \cos(x) - \cos(z) + \dfrac{4x + z - \cos(x) + \frac{y\sin(x)}{\cos(y)}}{2^{\cos(y)}y - 5\cos(y) + 13} - \dfrac{\sin(x)}{\cos(y)} + 8^{\cos(z)}\cos(x) + 1.953x10^6 \\[2mm]
q3 = z + 1.111x
\end{cases}
\tag{7}
$$

It is notorious that in both cases, the results were different. To visualize what the GP achieved in each case, Fig. 7a) shows case 1 with the model in (6), and Fig. 7b) shows case 2 with the model in (7). The chart shows the objective paths in circles in both cases, and the achieved paths in crosses.

In both cases, the results obtained by the GP tend to the requested path. However, it is essential to note that this soft search algorithm approximates the structure that meets the requested objective and does not optimize results, which is why it results in a similar path.

Table 2. Initial condition used in the GP algorithm.

Prove	Accumulated error of training	Accumulated error of testing
Case 1	4.599 mm	582.67 mm
Case 2	17.97 mm	154.13 mm
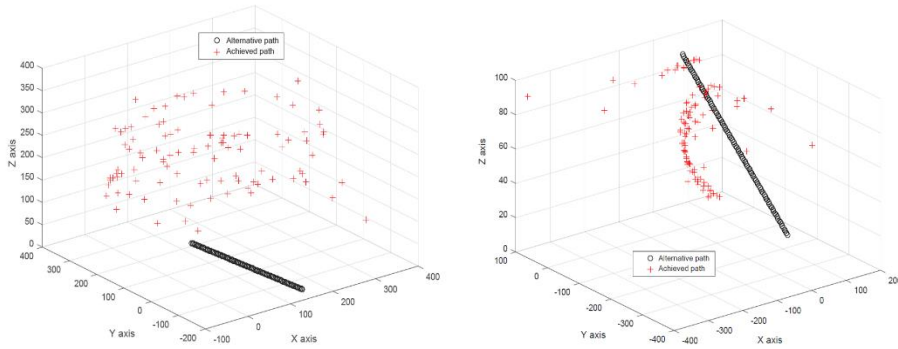
Fig. 8. a) Verification of results on an alternate route for case 1 b) Verification of results on an alternate route for case 2

These results are not conclusive but show that training requires several more points with an alternative path to produce an IK model.

Fig. 8a) shows case 1, and Fig. 8b) shows case 2 performances. It is identified from this analysis that the requested route in circles was not the route obtained by the robot in crosses.

Observing that the results are far away and different from the requested test route is verifiable by comparing the accumulated errors shown in Table 2. This way, the results are limited to the training routes.

It demonstrates the tendency to optimize the local minimum due to the lack of system information.

5 Conclusions

The tests carried out in this work demonstrate that a complex system such as a robotic arm requires several points to generate an IK model. Thus, soft search algorithms cannot consider all possible scenarios if there is no representative dataset of the search space. On the other hand, feeding the algorithm as poor information may reach a local minimum that follows the training path in the dataset used, i.e., the lack of information does not allow it to see the cases in which it fails.

In any case, the GP can solve this complex problem for specifically requested routes but fail in other scenarios.

These results are not an error and provide valuable information. Based on them, it is possible to identify the following failures extrapolated to any application. Moreover, it is vital to restrict the variables that affect the model and how they do it considering the third joint should not be a function of the x, y axes. On the other hand, is suggested a trying meshes of points with the expected resolution in the robot as a training dataset for future works using GP to obtain the IK model.

In the same way, the fitness function must contemplate a combinatorial of possible solutions to avoid that the GP disregards important points of work.

References

1. Barrientos, A., Peñil, L., Balaguer, C.: Fundamentos de Robótica (2007)
2. Baturone, A.O.: Robótica: Manipuladores y Robots Móviles. Marcombo (2005)
3. Bertram, D., Kuffner, J., Dillmann, R.: An Integrated Approach to Inverse Kinematics and Path Planning for Redundant Manipulators. In: International Conference on Robotics and Automation. ICRA, pp. 1874–1879 (2006) doi: 10.1109/ROBOT.2006.1641979.
4. Saha, S.K.: Introducción a la robótica. McGraw-Hill (2008)
5. Poli, R., Langdon, W.B., McPhee, N.F.: A Field Guide to Genetic Programming (With contributions by JR Koza) (2008)
6. Howard, L.M., D'Angelo, D.J.: The GA-P: A Genetic Algorithm and Genetic Programming Hybrid. IEEE Expert, 10(3), pp. 11–15 (1995) doi: 10.1109/64.393137.
7. Alfred, R.: Short-Term Time Series Modelling Forecasting Using Genetic Algorithm. In: Proceedings of the International Conference on Data Engineering (DaEng-2015), pp. 163–171 (2019) doi: 10.1007/978-981-13-1799-6_18.
8. Rivera, M.M., Ramos, M.A.P., Mora, J.L.O.: An Alternative Structure to Replace the Tree-Based Individuals in a Genetic Programming Algorithm for Decoupling MIMO Systems. In: 6th MICAI Workshop on Hybrid Intelligent Systems (2013)
9. Gao, Z., Wei, G., Dai, J.S.: Inverse Kinematics and Workspace Analysis of the Metamorphic Hand. Proceedings of the Institution of Mechanical Engineers Part C Journal of Mechanical Engineering Science, 229(5), pp. 965–975 (2015) doi: 10.1177/0954406214541429.
10. Nguyen, H.V., Le, T.D., Huynh, D.D.: Forward Kinematics of a Human-Arm System and Inverse Kinematics Using Vector Calculus. In: 14th International Conference on Control, Automation, Robotics and Vision (ICARCV), pp. 1–6 (2016) doi: 10.1109/ICARCV.2016.7838641.
11. Alibeigi, M., Rabiee, S., Ahmadabadi, M.N.: Inverse Kinematics Based Human Mimicking System Using Skeletal Tracking Technology. Journal of Intelligent and Robotic Systems, 85(1), pp. 27–45 (2017) doi: 10.1007/s10846-016-0384-6.
12. Duka, A.V.: ANFIS Based Solution to the Inverse Kinematics of a 3DOF Planar Manipulator. Procedia Technol, 19, pp. 526–533 (2015) doi: 10.1016/j.protcy.2015.02.075.
13. Raj, D.R., Raglend, I.J., Anand, M.D.: Inverse Kinematics Solution of a Five Joint Robot Using Feed Forward and Radial Basis Function Neural Network. In: International Conference on Computation of Power, Energy Information and Commuincation (ICCPEIC), pp. 117–122 (2015) doi: 10.1109/ICCPCT.2015.7159376.
14. Olaru, A., Olaru, S., Mihai, N.: Proper Smart Method of the Inverse Kinematic Problem. In:

Applied Mechanics and Materials, 772, pp. 455–460 (2015) doi: 10.4028/www.scientific.net/AMM.772.455.

15. Momani, S., Abo-Hammour, Z.S., Alsmadi, O.M.K.: Solution of Inverse Kinematics Problem Using Genetic Algorithms. Applied Mathematics Information Sciences, 10(1), pp. 225 (2016) doi: 10.18576/amis/100122.

16. Gupta, R.A., Chow, M.Y.: Overview of Networked Control Systems. In: Wang, F.Y., Liu, D.: Networked Control Systems. pp. 1–23 (2008) doi: 10.1007/978-1-84800-215-9_1.

17. Chapelle, F., Bidaud, P.: Closed Form Solutions for Inverse Kinematics Approximation of General 6R Manipulators. Mechanism and Machine Theory, 39(3), pp. 323–338 (2004) doi: 10.1016/j.mechmachtheory.2003.09.003.

18. Zhai, R., Wen, S., Zhu, J.: Trajectory Planning of NAO Robot Arm Based on Target Recognition. In: International Conference on Advanced Mechatronic Systems (ICAMechS), pp. 403–407 (2017)

19. Sadiq, A.T., Raheem, F.A.: Robot Arm Path Planning Using Modified Particle Swarm Optimization Based on D* Algorithm. Al-Khwarizmi Engineering Journal, 13(3), pp. 27–37 (2017) doi: 10.22153/kej.2017.02.001.

20. Becerra, Y., Arbulu, M., Soto, S.: A Comparison Among the Denavit-Hartenberg, the Screw Theory, and the Iterative Methods to Solve Inverse Kinematics for Assistant Robot Arm. In: International Conference on Swarm Intelligence, pp. 447–457 (2019) doi: 10.1007/978-3-030-26369-0_42.

21. Krastev, E.: Kinematic Path Control of a Redundant Robot Arm in Sliding Mode. In: International Conference on Robotics in Alpe-Adria Danube Region, pp. 281–288 (2017) doi: 10.1007/978-3-319-61276-8_31.

22. Praveena, P., Rakita, D., Mutlu, B.: User-Guided Offline Synthesis of Robot Arm Motion from 6-DoF Paths. In: International Conference on Robotics and Automation (ICRA), pp. 8825–8831 (2019) doi: 10.1109/ICRA.2019.8793483.

23. Michelin, M., Hervé, P.E., Tempier, O.: Path Following Demonstration of a Hybrid Cable-Driven Parallel Robot. In: International Conference on Cable-Driven Parallel Robots, pp. 323–335 (2021) doi: 10.1007/978-3-030-75789-2_26.

24. Boehm, J.R., Fey, N.P., Majewicz, A.: Inherent Kinematic Features of Dynamic Bimanual Path Following Tasks. IEEE Trans Human-Machine Syst., 50(6), pp. 613−622 (2020) doi: 10.1109/thms.2020.3016084.

25. Diaz, E., López, A.S., Serna, M.: Planificación reactiva de movimientos en tiempo real para robots móviles. Research in Computing Science, 147(7), pp. 115−128 (2018) doi: 10.13053/rcs-147-7-10

26. Gibbs, J.: Easy Inverse Kinematics Using Genetic Programming. In: Proceedings of the 1st Annual Conference on Genetic Programming, 422 (1996)

27. Chapelle, F., Bidaud, P.: A Closed Form for Inverse Kinematics Approximation of General 6R Manipulators Using Genetic Programming. In: International Conference on Robotics and Automation, ICRA, 4, pp. 3364−3369 (2001) doi: 10.1109/ROBOT.2001.933137.

28. Low, E.S., Ong, P., Cheah, K.C.: Solving the Optimal Path Planning of a Mobile Robot Using Improved Q-Learning. Robotics and Autonomous Systems, 115, pp. 143−161 (2019) doi: 10.1016/j.robot.2019.02.013.

29. Lavín-Delgado, J.E., Solís-Pérez, J.E., Gómez-Aguilar, J.F.: Trajectory Tracking Control Based on Non-Singular Fractional Derivatives for the PUMA 560 Robot Arm. Multibody

System Dynamics, 50(3), pp. 259–303 (2020) doi: 10.1007/s11044-020-09752-y.

30. Kalra, P., Prakash, N.R.: A Neuro-Genetic Algorithm Approach for Solving the Inverse Kinematics of Robotic Manipulators. In: International Conference on Systems, Man and Cybernetics, 2, pp. 1979–1984 (2003) doi: 10.1109/ICSMC.2003.1244702.

31. Rivera, M.M., Ochoa-Zezzatti, A., Ramírez, C.A.M.: Automatic Generation of Programs for Data Tables with Batch Least Square Mamdani Inference Systems: Application in the AWG Table. Research in Computing Science, 148(6), pp. 39–49 (2019) doi: 10.13053/rcs-148-6-3.

32. Sivanandam, S.N., Deepa, S.N.: Introduction to Genetic Algorithms. Science and Business Media (2007) doi: 10.1007/978-3-540-73190-0.

33. Torres, M.A.G., Ponomaryov, V.I.: Selección óptima de cartera de inversión de stocks de S&P 500: Uso de algoritmos genéticos. Research in Computing Science, 148(10), pp. 271–278 (2019) doi: 10.13053/rcs-148-10-23.

Comparative of Traffic Optimization with SUMO Using Genetic Algorithm and Particle Swarm Optimization

Martín Montes Rivera, Jorge Alonso Ramírez-Márquez,
Jesús Rafael Tavarez-Delgado

Universidad Politécnica de Aguascalientes,
Mexico

{martin.montes, jorge.ramirez, rafael.tavarez}@upa.edu.mx

Abstract. One of the main issues in urban transportation is traffic congestion, which wastes time and money resources. Aguascalientes city in Mexico is not an exception. Thus a research group integrated by Investel, Centro de Investigación en Matemáticas (CIMAT), Universidad Politécnica de Aguascalientes (UPA), among others has started build a solution for this type of problems. However, constructing new structures requiring a high investment is not always possible due to economic, demographic, and social reasons. As an alternative, traffic control techniques speed up vehicular traffic by controlling the time of traffic lights. Artificial intelligence is one approach to determining the optimal time for traffic light phases. In this work, we built a scenario with six traffic lights to test a Genetic Algorithm (GA) and Particle Swarm Optimization (PSO) to optimize traffic control as an initial step for the responsive control of Aguascalientes traffic lights. The optimization approach uses fitness and cost functions that measure the stopping time for each car in the traffic flow. Both optimization algorithms identify the necessary periods by evaluating candidate solutions with simulations performed by the SUMO platform, which considers traffic jams, car collisions, and time delays. Finally, we compare the GA and PSO (PSO), identifying the best algorithm in this scenario. The proposed method in this work will allow us to test several algorithms optimizing traffic lights phases for specific scenarios, which eventually help us with the appropriate sensors to generate responsive traffic lights in different road junctions in Aguascalientes, Mexico.

Keywords: Traffic lights optimization, simulation of urban mobility, GA, PSO, road traffic control.

1 Introduction

Transportation has been a critical issue within human civilization. One transportation problem is traffic congestion. Traffic congestion appears when too many vehicles use standard transport in infrastructure with a limited capacity [1]. Traffic congestion is a problem in several countries, including Mexico. However, a solution may be to build new roads; this is not always possible due to social, environmental, and economic

characteristics [2]. Aguascalientes, founded in 1575, is a state with an area of 5600 km2, located in the north-center of Mexico [3]. The urban mobility of Aguascalientes has grown since then, adding new parks, bikeways, vehicular bridges, and overpasses to deal with the increase of vehicles and pedestrian traffic flow [4]. Constructions presented in [5–8] support the construction of bridges and overpasses of the city, modifying the traffic to reduce the transportation time and maintaining the existing infrastructure for vehicles.

As an alternative to infrastructure, the systems for vehicular traffic control use diverse computer methods, and transport management methods use modern management systems with telecommunication technologies [9].

The primary control measure for urban land transport is traffic lights at intersections. The fundamental objective of traffic lights was initially to guarantee the safe crossing of vehicles and people [1]. However, due to the progressive increase in users, it has become necessary to establish the appropriate methodologies to make their use more efficient.

A simulation is the imitation of processes or systems in the real world. Also, a simulation is an indispensable methodology for testing the solutions and analyzing a system's behavior [10].

The traffic models for their simulation imitate traffic densities and average speeds [2]. Thus, these models allow generating focused strategies to improve vehicular traffic. In addition, computer simulations can point out the relation between the logical values of the problem and the decision-making system [11].

This article proposes a method for comparing algorithms optimizing traffic lights to reduce traffic congestion. We use two numerical optimization algorithms, Genetic Algorithms (GA) and Particle Swarm Optimization (PSO), the most representative of evolutionary and swarm intelligence algorithms, respectively. All simulations in this work use the Simulation of Urban Mobility (SUMO) platform.

SUMO is a traffic simulation software that allows modeling road vehicles, public transport, and pedestrians. Among the applications carried out with SUMO are evaluating traffic lights' performance and algorithms for their control [12].

Several investigations about the SUMO traffic simulations involve models for traffic demand and optimization in places such as Luxembourg, Medellin, Surabaya, Bologna, and Bandung Casablanca, Milan, and Samara [13–22]. Some of the characteristics of this software are that it is open-source, allows the simulation of cars, and contains tools to import road networks and generate routes from different sources to reproduce realistic mobility patterns.

The approach proposed in this work allows repeating the method for different crossroads with traffic lights in Aguascalientes, Mexico, towards developing a responsive vial control.

```
Input parameters: N_P, I_T, f(X_i), L_l, L_u, LS_l, LS_u, c_1, c_2, w
X_i=ψ_i ∈ [L_l,L_u];
V_i = 0;
C_i = f(X_i);
G_P = C_i;
G_B = min(G_B);
P_i = X_i;
P_G = X_argmin(f(X_i));
while  k < k_max  or  G_B ≤ C_d  do
    V_i = w · V_i + c_1 · R_1 · (P_G − X_i) + c_2 · R_2 · (P_i − X_i);   V_i = V_i ∈ [LS_l,LS_u] ;
    X_i = X_i + V_i; X_i = ψ_i ∈ [L_l,L_u];
    C_i = f(X_i);
    for i from 1 to I_T do
        if  G_P < C_i  then
            G_P = C_i;
            P_i = X_i;
        end
    end
    G_B = min(G_P);
    P_G = argmin(f(P_i));
end
```

Algorithm 1. PSO algorithm.

2   Theoretical Framework

2.1 Particle Swarm Optimization

The Particle Swarm Optimization algorithm (PSO) is a population-based optimization method developed in 1995 by James Kennedy and Russell Eberhart [23]. PSO mimics the nature and social behavior of organisms in groups, such as the motion of birds when they group in flocks, the motion of fish in schooling, and the ant colonies [24]. Nowadays, PSO has become a popular numerical optimization algorithm, and several variations using regrouping, neighborhoods, and unique parameters have been proposed [24–26]. However, in this work, we use the most common variant in proposed 1998 with inertial momentum [27].

The steps of PSO are in Algorithm 1. Its parameters include the minimum and maximum boundaries of the position of particles $X_i = \psi_i \in [L_l, L_u]$ ($[X_{min}, X_{max}]$), their velocities ($V_i = V_i \in [LS_l, LS_u]$) (initialized in zero); the inertial parameter (w), the maximum iterations (k_{max}), coefficients (c_1 and c_2) for personal and social components, the cost function $f(X_i)$, the cost value (C_i) of X_i, the best-known positions for each particle ($P_i = X_i$) , the global best cost G_B and the global best position ($P_G = X_{argmin(f(X_i))}$). The procedure iterates until I_T reaches k_{max} or finding the desired cost value (C_d) [27].

```
Input parameters: S_P, P, M_P, T_S, N_G, P_M
Create random population P
Evaluation of fitness (F)
while ending condition is not met, do
   Select individuals with the best F
   Crossover the selected individuals
   Mutate offspring from the crossover
   Evaluate F of new individuals
   Insert new individuals into the population
   Erase individuals with the worst F
End
Return individual with highest F
```

Algorithm 2. GA algorithm.
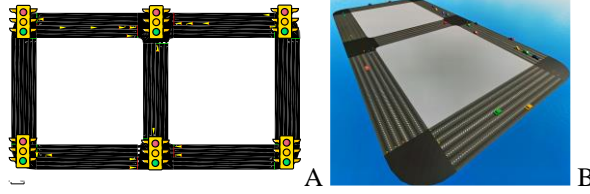
Fig. 1. Proposed Scenario. A: Schematic and B: Three-dimensional representations.

2.2 Genetic Algorithm

The genetic algorithm (GA) was developed between the 1960s and 1970s by John Holland, inspired by the natural selection principles proposed by Charles Darwin. The sections involved in the algorithm are population initialization, fitness calculation, crossover, mutation, and fitness selection [28–31].

Algorithm 2 describes GA. The GA parameters are population size (S_P), the tournament size (T_S), the number of generations (N_G), the mutation probability (P_M), the fitness function (F). The GA iterates until reaching the stopping conditions, such as the maximum generations N_G or the desired fitness value [32]. We use tournament selection, single-point crossover, and random mutation for this work.

3 Methodology

We start defining the optimization scenario using Python 3.8.10 with the last version of the SUMO library 1.1 and the plugging sumo-web3d 1.0. This scenario considers four possible situations in everyday crossroads with traffic lights: Go ahead, turn left, turn right, and U-turn. The map includes six crossroads with traffic lights, as shown in Fig. 1 for schematic and three-dimensional representations.

The traffic lights phases have two possible configurations. The first with states: 'GGGgGGGr,' 'yyyyyyyr,' 'GGGrGGGg,' and 'yyyryyyy.' The second with states: 'GGGgggrrrGGGGg', 'yyyyyyrrrryyyyy', 'rrrrrGGGgGrrrr', 'rrrrrryyyyyrrrr'.

The scenario proposed in Fig. 1 allows simulating complex behaviors in the SUMO library like:

- Covariance of traffic lights: Times for each traffic light depend on others.
- Traffic jams: Accumulation of cars when setting wrong traffic lights.
- Cars collisions: Accidents of cars when setting wrong times in the yellow light.
- Delay times: Cars must wait when the traffic light or a jam stops them.
- The vehicles' randomness: The decisions of cars at a crossroad are random.

3.1 Scenario Optimization with GA and PSO

Once the scenario was defined, we connected it with the optimization algorithms, following the definitions in sections 2.1 and 0. This implementation uses Python with the Traci library, which SUMO uses to manage connections to its simulator and access the resulting data.

The schema we used for optimizing the traffic scenario depends on numerical optimization, like the one performed with GAs and PSO. The parameters that the optimization algorithms tune were initially 24, which are the times for each phase of the six traffic lights on the map. However, we found that the phases that include yellow lights are constants in the optimization since they represent the required time for each driver to realize that the current light is about to change. Therefore, after eliminating each phase associated with the yellow light, we reduce the optimization to 12 dimensions, two phases per traffic light.

After identifying the parameters to optimize, we focus on the goal of this work, which is to optimize the times on traffic lights to reduce the stopped time for each car in the traffic flow.

Cost Function.

For preparing our optimization function, we consider reducing the vehicles' stopping time. Based on that idea, the accumulated stopped time for the vehicles indexed with i depends on the 12 times used in the phases on the traffic lights in the optimization, as shown in equation (1):

$$t_{s,i} = f(t_1, t_2, t_3, t_4, t_5, t_6, t_7, t_8, t_9, t_{10}, t_{12}). \tag{1}$$

Thus, our proposed cost function in equation (2) is the summation of all the vehicles' accumulated stopping times in the simulation. We will consider a minimizing problem in the optimization since the work goal is to reduce the stopping time:

$$Cost(t_1, t_2, t_3, t_4, t_5, t_6, t_7, t_8, t_9, t_{10}, t_{12}) = \sum_{i=1}^{n} t_{s,i}. \tag{2}$$

GA implementation.

Once the GA follows the definitions in section 0, we must configure its input parameters which include:

- Number of generations (N_G): We changed the parameter N_G to the number of evaluations (N_E). Because the GA and the PSO must evaluate the same number of

times the cost function to obtain a comparative result, the N_E, includes the evaluations used in the GA to generate the initial population and the evaluations of each generation. In this work, we set N_E=300, for 250 seconds per run in the GA.

- Population size (S_P). The population size affects the GA results since it represents the initial fitness evaluations to explore the search space [33]. Thus, we identify the best population size from 5-205 chromosomes with steps of 10 chromosomes or 1.66667% up to 68.33333% of the allowed cost function evaluations. Determining S_P with reliability implies different scenarios for validation and a technique for tunning like K-fold cross-validation. However, this is not the goal of the work, and we are interested only in this scenario. Therefore, when the scenario changes, we must repeat the tunning process.

- Tournament size (T_S). Tournament size affects the convergence speed in GAs, and a wrong value could result in premature convergence [33, 34]. Thus, we selected values from 3-100 chromosomes or crossover probability from 1% to 30% with steps of 5 chromosomes. We follow the same process described for S_P for determining T_S. Therefore, when the scenario changes, we must repeat the tunning process.

- Mutation Probability (P_M). The mutation mechanism helps introduce new information in GAs and avoid premature convergence. However, if P_M is high, an excess of noise affects the offspring. Thus, the literature recommends at much to 5% of probability [32]. Therefore we use 5% in this research.

The best GA parameters for our scenario test a total of 600 configurations for tournament size and the number of chromosomes.

PSO implementation.

Once the PSO follows the definitions in section 2.1. We must configure its input parameters which include:

- Number of iterations (I_T): We changed the parameter I_T to the number of evaluations (N_E). Because as mentioned before, PSO and GA must evaluate the same number of times the cost function to obtain a final comparative result. Again, we set the N_E=300, for 250 seconds per run. If the scenario changes, we must repeat the tunning process as mentioned in the GA implementation.

- Maximum values for the position [X_{min}, X_{max}]: We set them to [0.3,1.0], allowing reach the original from 30% to 100% of the original value. The minimum value selected allows avoiding cars collisions.

- Number of particles (N_P): Affects the PSO in the number of cost function evaluations per iteration. Thus, we identify bests values using 5-205 with steps of 10 particles, representing 1.66667% up to 68.33333% of the allowed evaluations. If the scenario changes, we must repeat the tunning process as mentioned in the GA.

- Inertial parameter (w): Intertial behavior allows controlling exploration of the search space like N_P with fixed N_E. Thus, we selected the best value in our scenario using 0.9-1.2 with steps of 0.1 units as recommended in the work that proposes this behavior.

- Personal and social components (c_1, c_2): We set these components equal to 2.0 as recommended by the original algorithm.

4 Results

This section shows all the algorithms and simulations we test in this work. The computer we used to carry out all the experiments is a Microsoft Windows 10 Pro system with an Intel(R) Core(TM) i7-6700 CPU @ 3.40GHz, 3401 Mhz with four central processors and RAM 16 GB, with motherboard ASUS Z170M-PLUS, and KINGSTON SUV400S37480G solid-state disk. All the results in this section consider the minimizing cost function proposed that measures the accumulated delay time for all the vehicles during the simulation, as mentioned in equation (2).

4.1 Results GA

We tested a total of 460 configurations with the GA in 30.39857 hours, with an average time of 237.90183 seconds per configuration, obtaining as the best result 33 seconds of accumulated delay time for 436 vehicles included in the SUMO simulation of 1000 seconds.

Fig. 2 shows the Surface Fitting, concerning the number of chromosomes, the tournament size, and the accumulated delay time for all the vehicles in the simulation. The blue values are the best ones with lower accumulated delay time. The best configuration is in the blue point at $(S_p = 85, Ts = 58, BestFitness = 33)$.
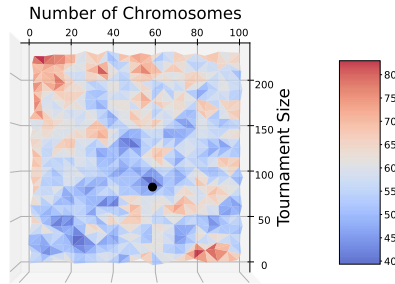
Fig. 2. Surface with all configurations for the GA and its fitness. Best configuration $(S_p = 85, Ts = 58, BestFitness = 33)$.

Fig. 3 shows the worst and best fitness across generations, in red and blue, respectively, for the GA's best configuration. The charts' generations are 110 since the algorithm stops after 300 fitness evaluations, as stated in section 3.1.
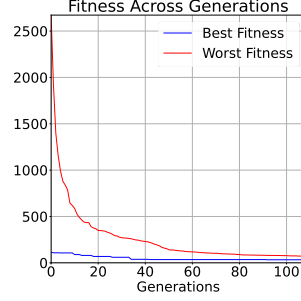
Fig. 3. Fitness across generations for the GA with the best configuration.

Table 1 shows the times of the best candidate solution of GA, including the two phases duration (phase of green light and phase of red light) on each of the six traffic lights in our scenario. This configuration produces 33 seconds of delay for 436 vehicles in 1000 seconds of simulation in SUMO.

Table 1. Time in phases for each traffic light obtained with the GA best candidate solution using the best configuration ($S_p = 85, Ts = 58, BestFitness = 33$).

Traffic Light	Phase with Green Light (seconds)	Phase with Red Light (seconds)
1	27.15134865	29.84865135
2	41.18746251	15.81253749
3	27.17673005	29.82326995
4	41.15427277	15.84572723
5	41.66752012	15.33247988
6	22.2938168	34.7061832

4.2 Results PSO

We tested a total of 69 configurations with the GA in 5.38600 hours, with an average time of 281.00336 seconds per configuration, obtaining as the best result 15 seconds of accumulated delay time for 436 vehicles included in the SUMO simulation of 1000 seconds.

Fig. 4 shows the Surface Fitting, concerning the number of particles, the inertial coefficient, and the accumulated delay time. Blue values are the best ones with lower accumulated delay time. The best configuration is in the blue point ($N_P = 55, w = 0.9, BestCost = 15$).
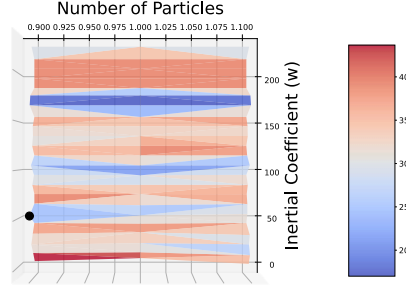
Fig. 4. Surface with all configurations for the PSO. Best configuration is ($N_P = 55, w = 0.9, BestCost = 15$).

Fig. 5 shows the worst and best cost across iterations, in red and blue, respectively, for the best configuration obtained in our scenario using the PSO. The charts' generations are five since the algorithm stops at this point after 300 fitness evaluations, as stated in section 3.1 for applying the same cost evaluations in GA and PSO algorithms.
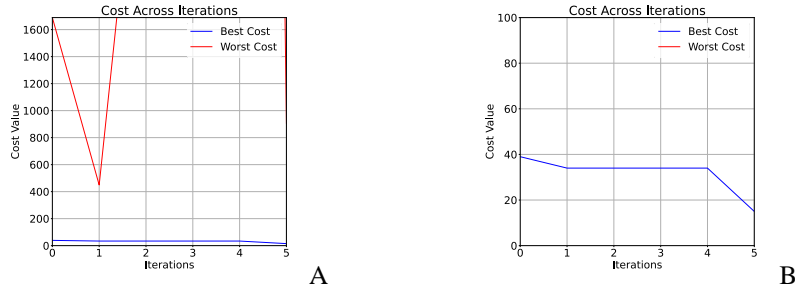
Fig. 5. Cost across iterations for the PSO with the best configuration. A: window between the worst initial cost and the best cost. B: window between the best initial cost and the best cost.

4.3 Comparison of GA and PSO Results

In this work, we are interested in determining the best algorithm to optimize times in traffic lights using the SUMO library for our proposed scenario with six traffic lights. We test the algorithms and evaluate them based on two critical variables, quality of best solution and execution time for obtaining it. Since we evaluated more GA than PSO configurations, the comparison results in this section consider only the best 30 configurations randomly sampled from GA and PSO configurations.

Fig. 6 Shows two box plots obtained from 30 random samples of the tried configurations. The first one (A) considers the fitness and cost values, and the second one (B) considers the execution times.

A box plot shows that the GA fitness has a lower variance than the cost value of the PSO when varying its parameters. However, the PSO obtained better quality solutions than GA in the majority of the configurations.

B box plot shows a lower variance in execution times per generation in the GA than in iterations of the PSO. However, this is related to how the algorithm works; the number of particles changes the number of simulations carried out by SUMO per iteration. On the other hand, changing the number of chromosomes or the mutation percentage does not modify the GA's number of simulations per iteration.
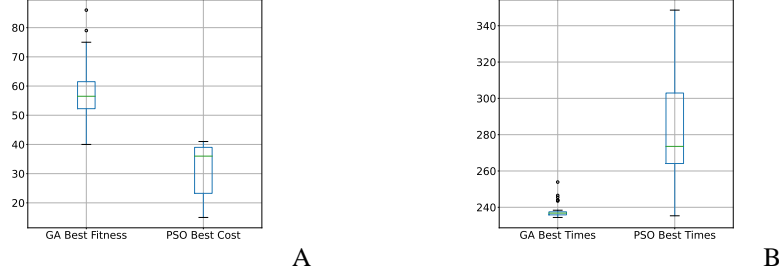
Fig. 6. Comparison between GA and PSO algorithms with 30 random samples of the tried configurations. A: Comparison between fitness and cost values. B: Comparison between execution times.

After analyzing the box plot comparisons, we found that PSO produces better quality solutions than GA, but it requires more time per simulation for doing it. Even though PSO requires more time per iteration, we base our analysis on cost evaluations in this study. Thus, we reduce the number of iterations by increasing the number of particles, and even with that, the PSO produces better quality solutions. The ANOVA test in **Table 2** supports better quality solutions of PSO, with F-score = 102.95786 and P-value = 1.803639E-14, and lower execution times in GA, with F-score = 62.66525 and P-value = 8.46629E-11.

Table 2. Values of validation for the conclusion based on ANOVA.

ANOVA values	Fitness and Cost values.	Execution times in GA and PSO.
F-score	102.95786	62.66525
P-value	1.803639E-14	8.46629E-11

5   Conclusions

This work compares the GA with the PSO algorithm in quality and execution times when optimizing delay times of vehicles by changing phase times on traffic lights, which are crucial when optimizing traffic light controllers. All the algorithms and simulations we carry out use Python as a programming language with the open-source SUMO (Simulation of Urban Mobility) library.

We use the accumulated delay in cars in a SUMO simulation to optimize the times of traffic lights. We test the variation of input parameters on each algorithm and simulate their results, maintaining 300 as the maximum number of cost evaluations.

As a result, we found that PSO produces better quality solutions than the GA but requires more time per iteration when optimizing. However, we reduced the number

of iterations by increasing the number of particles, basing our analysis, but the PSO remains obtaining the best quality solutions.

We support our analysis on box plots with the ANOVA test, obtaining that the PSO has better quality solutions, with F-score = 102.95786 and P-value = 1.803639E-14. The GA has lower execution times per iteration, with F-score = 62.66525 and P-value = 8.46629E-11.

The main contribution of our work is a methodology for optimizing traffic lights based on accumulated delay times. First, we evaluate the results of the proposed method on a specific scenario.

5.1 Future Work

In this work, we probe sufficient evidence that the PSO produces better results in optimizing traffic lights for a specific scenario. However, both algorithms must test several more scenarios to support that one is better than the other. On the other hand, other algorithms could test our approach.

References

1. Papageorgiou, M.: Overview of Road Traffic Control Strategies. IFAC Proc. Vol. 37, 29–40 (2004). https://doi.org/10.1016/S1474-6670(17)30657-2.
2. Bellemans, T., De Schutter, B., De Moor, B., Bellemans, T., De Schutter, B., De Moor, B.: Models for traffic control. Delft Univ. Technol. Fac. Inf. Technol. Syst. J. A. 43, 13–22 (2002).
3. Gómez Serrano, J., Delgado Aguilar, F.J.: Aguascalientes: Historia breve. Fondo de Cultura Económica, Mexico City (2016).
4. H. Ayuntamiento de Aguascalientes 2019-2021: INICIA MUNICIPIO OBRAS DE REHABILITACIÓN DE LA AVENIDA MARIANO HIDALGO.
5. Dávalos, T.: Anuncian más obras públicas para Aguascalientes - El Sol del Centro | Noticias Locales, Policiacas, sobre México, Aguascalientes y el Mundo.
6. Granados, F.: ¿Qué sigue para la movilidad urbana en Aguascalientes?/ Agenda urbana - LJA Aguascalientes.
7. Newsweek: Inician obras de construcción de paso a desnivel de Av. Aguascalientes y Fracc. Parras | Newsweek México.
8. Flores Nieves, A.J.: Pendiente en Aguascalientes, el próximo puente en Barberena Vega - LJA Aguascalientes.
9. Pamula, T.: Road traffic parameters prediction in urban traffic management systems using neural networks. Transp. Probl. 6, 123–128 (2011).
10. Banks, J.: Introduction to simulation. WSC'99. 1999 Winter Simul. Conf. Proc. 1, 7–13 (1999). https://doi.org/10.1109/WSC.1999.823046.
11. Fedorko, G., Rosova, A., Molnár, V.: The application of computer simulation in solving traffic problems in the urban traffic management in Slovakia. Theor. Empir. Res. Urban Manag. 9, (2014).

12. Alvarez Lopez, P., Behrisch, M., Bieker-Walz, L., Erdmann, J., Flötteröd, Y.-P., Hilbrich, R., Lücken, L., Rummel, J., Wagner, P., Wießner, E.: Microscopic Traffic Simulation using SUMO. 2019 IEEE Intell. Transp. Syst. Conf. 2575–2582 (2018).

13. Krajzewicz, D.: Traffic Simulation with SUMO – Simulation of Urban Mobility. Int. Ser. Oper. Res. Manag. Sci. 145, 269–293 (2010). https://doi.org/10.1007/978-1-4419-6142-6_7.

14. Codeca, L., Frank, R., Faye, S., Engel, T.: Luxembourg SUMO Traffic (LuST) Scenario: Traffic Demand Evaluation. IEEE Intell. Transp. Syst. Mag. 9, 52–63 (2017). https://doi.org/10.1109/MITS.2017.2666585.

15. Acosta, A.F., Espinosa, J.E., Espinosa, J.: Application of the SCRUM Software Methodology for Extending Simulation of Urban MObility (SUMO) Tools. In: Simulating Urban Traffic Scenarios. pp. 3–15. Springer, Cham (2019). https://doi.org/10.1007/978-3-319-33616-9_1.

16. Dian Khumara, M.A., Fauziyyah, L., Kristalina, P.: Estimation of Urban Traffic State Using Simulation of Urban Mobility(SUMO) to Optimize Intelligent Transport System in Smart City. 2018 Int. Electron. Symp. Eng. Technol. Appl. IES-ETA 2018 - Proc. 163–169 (2019). https://doi.org/10.1109/ELECSYM.2018.8615508.

17. Bedogni, L., Gramaglia, M., Vesco, A., Fiore, M., Härri, J., Ferrero, F.: The Bologna ringway dataset: Improving road network conversion in SUMO and validating urban mobility via navigation services. IEEE Trans. Veh. Technol. 64, 5464–5476 (2015). https://doi.org/10.1109/TVT.2015.2475608.

18. Aditya, F., Nasution, S.M., Virgono, A.: Traffic Flow Prediction Using SUMO Application with K-Nearest Neighbor (KNN) Method. Int. J. Integr. Eng. 12, (2020).

19. HRIMECH, H., BENALLA, M., ACHCHAB, B., EL ALAOUI, A., EL HAIL, M.: Simulation optimization using SUMO: case of Casablanca. Int. J. Comput. Eng. Data Sci. 1, 28–36 (2021).

20. Alazzawi, S., Hummel, M., Kordt, P., Sickenberger, T., Wieseotte, C., Wohak, O.: Simulating the Impact of Shared, Autonomous Vehicles on Urban Mobility – a Case Study of Milan. Epic Ser. Eng. 2, 94–110 (2018). https://doi.org/10.29007/2N4H.

21. Golovnin, O.K., Pupynin, K. V., Privalov, A.S.: A Web-Oriented Approach for Urban Road Traffic Simulation. 2019 Int. Multi-Conference Ind. Eng. Mod. Technol. FarEastCon 2019. (2019). https://doi.org/10.1109/FAREASTCON.2019.8934302.

22. Maiorov, E.R., Ludan, I.R., Motta, J.D., Saprykin, O.N.: Developing a microscopic city model in SUMO simulation system. J. Phys. Conf. Ser. 1368, 042081 (2019). https://doi.org/10.1088/1742-6596/1368/4/042081.

23. Lu, H., Chen, J., Guo, L.: Energy Quality Management. In: Comprehensive Energy Systems. pp. 258–314. Elsevier (2018). https://doi.org/10.1016/B978-0-12-809597-3.00521-6.

24. Lindfield, G., Penny, J.: Particle Swarm Optimization Algorithms. In: Introduction to Nature-Inspired Optimization. pp. 49–68. Academic Press

(2017). https://doi.org/10.1016/B978-0-12-803636-5.00003-7.

25. Evers, G.I., Ghalia, M. Ben: Regrouping particle swarm optimization: A new global optimization algorithm with improved performance consistency across benchmarks. 2009 IEEE Int. Conf. Syst. Man Cybern. 3901–3908 (2009). https://doi.org/10.1109/ICSMC.2009.5346625.

26. Kennedy, J.: Small worlds and mega-minds: effects of neighborhood topology on particle swarm performance. In: Evolutionary Computation, 1999. CEC 99. Proceedings of the 1999 Congress on. pp. 1931–1938 (1999). https://doi.org/10.1109/CEC.1999.785509.

27. Sun, J., Lai, C.H., Wu, X.J.: Particle Swarm Optimisation: Classical and Quantum Perspectives. CRC Press (2016).

28. Yang, X.-S.: Genetic Algorithms. Nature-Inspired Optim. Algorithms. 91–100 (2021). https://doi.org/10.1016/B978-0-12-821986-7.00013-5.

29. Rojas, M.H.G., Arellano, H.V., González, D.U., Rivera, M.M., Justo, M.O.A.: Steering Wheel Control in Lane Departure Warning System. Res. Comput. Sci. 2, 9–21 (2018).

30. Ramírez, C.A.M., Rivera, M.M.: Optimization of a Production Process from Demand and Number of Defective Units through Diffused Logic and Genetic Algorithms. Res. Comput. Sci. 2, 109–118 (2018).

31. Díaz-Nacar, E., Rodríguez-Vázquez, K.: Implementación en hardware de un algoritmo genético para resolver un problema combinatorio. Res. Comput. Sci. 8, 379–392 (2020).

32. Weise, T.: Global Optimization Algorithms - Theory And Application. (2009).

33. Weise, T.: Global optimization algorithms-theory and application. (2009).

34. Montes Rivera, M., Padilla Díaz, A., Ponce Gallegos, J.C., Canul-Reich, J., Ochoa Zezzatti, A., Meza de Luna, M.A.: Performance of Human Proposed Equations, Genetic Programming Equations, and Artificial Neural Networks in a Real-Time Color Labeling Assistant for the Colorblind. In: Martínez-Villaseñor, L., Batyrshin, I., and Marín-Hernández, A. (eds.) Advances in Soft Computing. pp. 557–578. Springer International Publishing, Cham (2019). https://doi.org/10.1007/978-3-030-33749-0.

Mental fatigue analysis in an Industry 4.0 workstation using an intelligent R language-based model

Andrés Esquivias-Varela [1] Humberto García-Castellanos [2] Alberto Ochoa-Zezzatti[3]

1 Tecnológico Nacional de México IT Ciudad Juárez, Chih. México
Student in Engineering Sciences PhD
aesquivias6@gmail.com
2 Tecnológico Nacional de México IT Ciudad Juárez, Chih. México
Engineering Sciences PhD
humber.gc@cdjuarez.tecnm.mx
3 Autonomous University of Ciudad Juarez, Chih. México
Research at Technology PhD
alberto.ochoa@uacj.mx

Abstract. Nowadays, it is common to present mental fatigue, which would decrease the physical and psychological capacity for developing a job. This effect leads us to the work stress presented by workers in Industry 4.0. It showed these two effects to a drop-in labor efficiency of workers and, in turn, impacting the productivity of the same, which represents production losses for the industry, considering the physical and psychological health of the users in their work environment. Mental fatigue implies the attention of the company's personnel to correct and prevent the problem.

The article represents analysis in a workgroup, which is processed information based on questionnaires to staff that seeks to find the effect of mental fatigue according to their work activities. In turn, it aims to find a faster analysis through digital virtualization and representation in virtual images to process the information captured in real-time. In this way, it will be possible to offer a better work environment to avoid the mental fatigue of workers and thus not affect their productivity and mental health.

Keywords: Psychosocial risk, Analysis, Fatigue, Productivity, Virtualization.

1   Introduction

Within the industry and under the new ways of working of Industry 4.0 imply that working methods refer to the path of work execution and the work environment surrounding the workers. Interaction plays a significant role in the climate of modern industries, where different and diverse types of work techniques help the idea of working in a fatigue-free environment. The physical environments of sectors are designed to simplify collaboration through a higher visual and psychosocial level. Scientific studies have analyzed the difficulties of performing mentally taxing tasks in the modern industrial environment. They are complying with Mexican Standards, especially NOM-035, implemented since 2018 at a national level, which is a regulation issued by the Ministry of Labor and Social Welfare. Which aims to identify, analyze and prevent psychosocial risk factors, workplace violence through separate agreements and regulations, both

national and international, that Mexico has ratified in labor justice, competitiveness, and trade, to promote a favorable organizational environment in workplaces [1].

In 2016, the International Labor Organization OIT reported on Psychosocial Risk Factors (PRF) and determined that they are a global problem that causes conflict in the professions and all users in any work environment.

It is determining that Psychosocial Risk Factors (PRF) are present in the workplace and concluding that it is the best place to prevent and act on them, to ensure the health and welfare of workers.

We must understand the difference between PRF and RP. We can appreciate factors as causes/conditions and risks as consequences. Psychosocial risk factors (PRF) are the characteristics of working conditions, especially the characteristics of their organization, affect people's health through psychological and physiological mechanisms that we also call stressors, intertwined with each other:

- Environmental working conditions.
- The need to exceed capabilities.
- Degree of responsibility and psychological burden.
- Lack of work autonomy.
- Time, rhythm, and work schedule.
- The function and content of the task are not clearly defined.
- Conflict between family and work relationship.
- Method of command and communication.
- Harassment, discrimination, and violence.

Psychosocial risk (PSR) is the negative psychological, physical, and social consequences caused by deficiencies in the design, organization, and management of work. The most common are:

- Acute and chronic work stress.
- Absenteeism
- Survivor syndrome
- Burnout/boredom syndrome (job burnout syndrome)
- Work addiction
- Bullying (workplace harassment)
- Violence, harassment, and discrimination
- Pain, depression, somatization

2   Related Literature

In the workplace, most studies examine the behavior and performance of employees in the activities to be performed, considering the complexity of learning and executing these activities. The literature analyzes three groups of small, medium, and extensive activities with the same difficulty.

De Croon et al. conceptual model [2] Two sets of parameters are analyzed: office philosophy and working conditions, which affect workers' short-term physical and psychological responses and long-term health and performance.
The concept of efficiency affects working conditions, including job requirements (cognitive load, workload, and workday) and job resources (communication, job autonomy, privacy, interpersonal relationships) [2].

To fully understand the impact of the work environment, other aspects that affect employee satisfaction, like the importance of furniture, quality of IT facilities, lighting, air quality, etc., must be considered. These factors affect the health and performance of employees, color, and material [2]. Saidi et al. [3]. Participants completed the test under normal working and quiet (off-work) conditions. The researchers found that although the memory performance of the smaller open area compares to the larger open space, cognitive performance: the number of interruptions (human and virtual) has a more significant impact on cognitive performance than the number of employees and virtual interruptions.

Psychological causes such as antipathy, discouragement, anguish, and job displacement appear to be related to physical health, especially heart disease. [4,5]. The unfavorable hazard status in psychological aspects seems categorized as a general social disadvantage. [6,7] Accordingly, the " psychosocial assumption" suggests that psychosocial stressors are an essential contributor to health disparity [8]. Those contributors involve numerous states of mind, psychological features, or aspects of health inequality. With a derogatory meaning. This article considers "psychosocial factors" for any physical health outcome that may affect physical health through psychological mechanisms—revisiting critically the emerging proof that a causal association causes the relationship between psychosocial stressors and physical well-being.

If this is not causal, it is unlikely that targeted psychosocial exposure interventions will benefit population health. An agreement reached that the results of the tests are sufficient to form the basis for health policy should come from health policy and should come from controlled trials of interventions that can change the relevant exposure and assess the impact of that exposure. Manipulate to guide health outcomes [6]. In some cases, this method is so. In some cases, this method is impractical or unlikely to be adopted for other reasons [5].

3   Methods

Recruit 33 workers aged 24 ± 5 years (3 classes, 28 men) and 24 ± 5 years (5 women). Recruit only workers without cognitive impairment or recent physical injury. Each participant completed a psychological assessment questionnaire, which included production lines in the automotive industry and workstations:
  - Company selection
  - Design pattern implementation

4

    - Prototyping - Cutting Accuracy
    - Time to design a prototype
    - Difficult to follow design rules of design
    - Difficult to generate the creativity required
    - Difficult to organize the prototype
    - Final course rating

All participants also reported normal or corrected vision and described themselves as being able to answer the questionnaire. The research was in a company specializing in seat fabrics for the automotive industry in Ciudad Juarez, Chihuahua, Mexico.

3.1   Measurements

Considering a set of work performance variables including different nominative categories, such as gender, age, and shift of workers, we used three classifiers (Bayesian network, random forest, and neural network-perceptron). We analyzed the performance algorithm of each classifier; it was used to establish a set of suitable indicators that will produce promising results in the main aspects related to mental fatigue.

Each algorithm can correctly classify more than two-thirds of the data set (dataset), which is the decisive element in finding the group and factors related to overwork. Due to the pressure to increase the number of parts, the male group continues to perform activities but considers that quality declines. In contrast, in the female group, quality is prioritized, where production is raised and minimizes delays, especially when using laser cutting plans. This tool is not as bold as a drill but has greater precision and adaptability in the cutting method and its accuracy in producing parts. However, among the vehicle objects, the female group is more detailed than the male sample, and the female group is only interested in mass production. Factors such as age, gender, and shifts also show significant differences in work performance, hence in the mental fatigue of each worker. The article is based on the analysis of a working group, which seeks the effect of mental fatigue according to their work activities in which will be measured: Selection of the company, implementation of the design pattern, prototyping - cutting, accuracy in cutting, the average time to design a prototype, difficulty in following the rules of design, difficulty in generating the required creativity, difficulty in organizing the prototype, average rating, end of the course, where the sum of the factors of each of the measures will have to give us a rating of 10 at its highest point, with these ratings and subdivisions. We will be able to understand better the areas in which the improvement issues will have evaluated to achieve optimal product production without having a difference in gender, age, and shift schedules. Figure 1 shows the data captured for the analysis in this study.

	Company selection	Design pattern implementation	Prototyping - Cutting Accuracy	Precision in Cutting	Average	Time to design a prototype	Difficult to follow design rules of design	Difficult to generate the creativity required	Difficult to organize the prototype	Average	Final course rating
First working shift											
141021 RUÍZ GALLEGOS ÁNGEL	5.9	2.1	3.7	3.6	3.8	1.8	2	1.6	5.4	2.7	9.3
153148 HERNANDEZ SANCHEZ DANIELA VALERIA	4	5.4	5.7	3.4	4.6	1.5	4	1.9	6.8	3.5	8.1
154665 HERNÁNDEZ ANTILLÓN JEAN OLIVER	5.7	4.1	3.4	6.5	4.9	6.2	5.3	4.4	1.5	4.3	9.4
154780 NORIEGA ANGULO RUBÉN	3.8	2.1	4.1	2.5	3.1	4.5	3.9	6.3	3.4	4.5	7.9
158790 GALLEGOS BORUNDA FERNANDO HUMBERTO	6.2	2.5	6.5	4	4.8	3.9	2.6	6.7	1	3.5	8.1
162988 MADRID DIAZ DE LEON JULIAN ANDRES	5.2	5.5	6.4	6.2	5.8	3	5.7	4.2	4.5	4.3	8.5
163010 HOLGUIN HERNANDEZ ROBERTO	3.1	3.3	6	6.8	4.8	6.5	2.7	6.6	3.8	4.9	8
163023 SOTO QUIROZ PEDRO	4.6	3.2	4.5	3.8	4	4.2	3.7	2.9	5.3	4	9.6
163037 RODRIGUEZ CABRALES ANGEL DE JESUS	2.4	2.4	1.5	2.8	2.3	3.1	5.8	7	2.1	4.5	8
168792 DÍAZ DOMÍNGUEZ CARLOS OMAR	1.6	2.2	2.8	4.7	2.8	6.9	3.6	2.1	7	4.9	9.2
Second working shift											
155986 CORRAL MELÉNDEZ ERIC ARIEL	5	1.6	5.5	5.7	4.4	1.9	3.5	5.3	6.2	4.2	8.4
162974 FRAIRE MEJIA JOSE ANGEL	3.5	4.4	5.3	5.3	4.6	2	5.1	5.4	3.7	4	9.4
168768 ESPINOSA PERALES JORGE ANIBAL	1	4.7	6.6	4	4.1	2.9	6	4	5	4.4	8.3
168836 HERRERA GONZÁLEZ HÉCTOR ARMANDO	5.2	4.8	4.7	4.9	4.9	6.7	6.2	4	5	5.5	8.2
169038 GOMEZ ALVARADO BALTAZAR ANTONIO	2.4	3.2	3.7	6	3.8	2.6	5.6	2.1	2.7	3.2	9.1
172126 REYES PENAGOS ISIS ARIADNA	1.8	1.2	5.3	6.2	3.6	4.1	5.5	4.9	3.4	4.5	9.5
179709 QUEZADA MEDINA PEDRO ARMANDO	5.3	1.4	6.4	6.2	4.8	1.2	1.9	3.5	5.4	3	8.8
179748 QUIROZ MEDRANO THOMAS ANTONIO	2.5	5.4	5.1	4.2	4.3	6.9	1.9	6.1	6.1	5.3	9.1
179810 AGUILAR AVILA ERICK EDMUNDO	5.1	1.4	2.9	2	2.9	4.2	4.4	4.8	6.3	4.7	9.3
179846 BERTHELY GONZÁLEZ EVELYN	4.7	6.9	6.3	5	5.7	1.1	6.7	6.1	2.6	4.1	8.3
182080 SOLEDAD ZEPEDA RAUL ISAAC	6.7	1.8	5.8	3	4.3	4.7	3	1.3	3.1	3	9.3
Third working shift											
145429 MUÑOZ PEREZ JONATHAN	2.2	6.5	2.2	6.3	4.3	2.8	1.9	2.1	1.6	2.1	8.5
154684 MONTOYA JAQUEZ LUIS OMAR	3.9	4.8	5.8	2.8	4.3	5.3	1.6	3.2	5.7	4	8.4
168701 LOPEZ MONTOYA FABIAN	4.3	1.5	5.2	5	4	6.4	5.7	5.1	4.9	5.5	9.6
172087 RIVERA HERNANDEZ ALEXIS MICHELLE	6.1	3.4	1.3	4.4	3.8	6.6	3.7	6.2	4.8	5.3	8.2
172095 APODACA JUÁREZ JESÚS ADRIÁN	3.3	4.7	3.3	5.5	4.2	2.7	2.9	5.6	5.7	4.2	8.7
172127 MOTA MEDINA MISAEL IGNACIO	3.6	2.4	2.3	4.6	3.2	6.7	3.7	3.2	5.3	4.7	9.6
172156 RUVALCABA DE LA FUENTE CÉSAR	1.3	2.8	4.3	2.7	3	1.8	5.5	6.2	4.1	4.9	8.9
179758 MENDOZA SOSA NAOMI GUADALUPE	5.2	1.5	4.5	1.4	3.1	5.4	5.1	6	3.3	5	8.2
179798 SILVA AGUIRRE SAMUEL	4.9	5.7	5.1	1.7	4.4	6.8	6.6	6.3	5.7	6.3	9.7
179813 CARMONA MARTINEZ CARLOS DANIEL	4.2	1.9	2.2	4.4	3.2	5.7	4.7	3.4	5	4.7	7.9
182568 CHAVEZ VELAZQUEZ ALAN GERARDO	1.4	2.5	6.8	4.1	3.7	2.8	4	4.9	4	3.9	8.2
185442 MONROY AGUIRRE DIEGO ALEJANDRO	2.3	4.5	4	3.7	3.6	6.8	4	2.3	1.7	3.7	9.4

Fig. 1. Data capture of workers in different work shifts

3.2 Description of used algorithms

In the next part of the survey, the three algorithms used will be described, and the numbers related to the performance of each algorithm will be shown in terms of their main characteristics and correctly characterized by this survey:

Naive Bayes Supposes that the occurrence or lack of a given feature is not linked to the event or lack of any other component. Its classifications are based on probability. In general, the Naive Bayes model is a machine learning algorithm for data classification. This algorithm is based on a statistical classification technique called "Bayes' Theorem." This algorithm is one of the simplest algorithms and has a great capacity to perform classification on large data sets. A Bayesian classifier works to assume that a feature taken from a class is independent of the different components extracted. Taking

as an example the application for a bank loan by a specific person, it will be granted depending on other factors such as his loan history, monthly or biweekly income, location, age, and even his occupation where although the conclusion depends on all these characteristics, the Bayesian classifier deals with it independently, that is why it is called naïve.

This classifier has excellent advantages such as its ease of implementation and the speed with which it predicts a class or label within a dataset likewise; by having some independence in its characteristics, it works with a success rate and requires a smaller amount of data for training. However, it also has several disadvantages; the first is known as zero probability. If the training data set does not have a category found within the test data set. It cannot make any prediction, and he ends up developing a probability of 0. The second significant advantage is the limited application to real-world problems. The benefit is almost impossible to obtain a set of fully independent predictors. To execute the Naive Bayes classifier within this research, Naïve Bayes Classifier was implemented as part of the Text Blob library, which is used for textual data processing within the Python environment. This library has several applications such as spelling corrections, word frequency, or in this particular case, sentiment analysis.

The series of sentences declared within the Python script was used. The sentences that are used as training sets are obtained from a JSON file, although in some other circumstances, they can also be obtained from an Excel file. In this file extracted from Python are the various phrases, along with the label of the emotion given by the same human analysis during the pre-processing stage of the data. After performing the execution, labeling is consistent with the various emotions initially established. The implementation of the Naive Bayes algorithm is less extensive in terms of code, unlike the rest of the algorithms implemented in this research. However, it requires a well-selected bag of phrases for the JSON file because this makes the difference between a good classification or one with low success.

Neural Networks The primary goal of this model is to learn by modifying itself automatically to perform complex tasks that could not be carried by classical rule-based programming. The network receives a set of incoming data, and each of these feeds arrives at a node named neuron. The neurons in the network are arranged into layers that make up the neural network. Each neuron in the network has a value, a weight and uses it to change the incoming value. The new value gained leaves the neuron and continues through the web. The algorithm outputs a rating instead of a probability. It seeks to "learn" from examples of what can be adjudicated by a label (class) but not what is not (this sorter does not try to determine the definition of a sentence but to rank it).

It is possible to determine that classes with large training sets are present; this can create distorted classification scores, which forces the algorithm. To adjust the scores relative to the size of the class (not ideal as its equivalent in an actual situation would be when a person is forced to decide in an ipso facto manner). The researcher uses a natural language toolkit to develop this method. Because it was required to find a way to convert the phrases into words accurately and reliably derive them, it is then

necessary to input the data into a training array, making sure to input the corresponding sentences along with their associated emotion.

Once you have all the data, you now need to organize the training data to identify sentences, classes, and the words that you can find within the sentences to determine a word bank and derive unique expressions. The derivation helps the network to match words such as "power" (force) and "power" (permission) to exclude the context where they are used. Since each sentence in training is reduced to a matrix of 0's and 1's, it can identify the unique words in the corpus.

It also allows to determine or associate this matrix within a class. Still, consider that a sentence can have several types or none at all. (this usually happens when there is a sentence whose reaction is unique and could not be interpreted previously in training or when it has no meaning at all, as if we were trying to make the network try to understand "asdfghjkl"). The function to standardize the values and their derivative was used to estimate the error rate. Repeat and adjust up to an acceptable low error rate. A problem also arose when implementing the bag of words since its unique character was required. For training, ten neurons were used within the hidden layers and put through 10000 epochs. It is considering that this allows better to classify the sentences with a reasonable error rate. It is configured inside a JSON file to store the synaptic weights (those that define the connection strength between two neurons). Once you have the model, it is possible to "predict" a new sentence that has not been described before and generate the probability of belonging to one of the classes. During the realization of this project, in the feature selection to improve the model. The test requires verifying the predictions in each case since, for an extensive dataset, it could take a considerable amount of time to check if there is some parameter that allows establishing some confidence with the user. Some prediction situations demand more reliability than others, and not all text categorization scenarios are equivalent to others.

Random Forest A Random Forest is a set of decision trees combined with bagging. When bagging is used, what happens is that different trees look to varying portions of the data; no single tree sees all the training data, so each tree is trained with varying samples of data for the same problem. Thus, by combining their results, some errors are compensated with others, and we have a generalized prediction with a better result. The characteristics selected after each training, the set of trees chosen can vary, having better or worse accuracy than the last time, for the exercise of this system.
The texts require pre-processing before training the system. The texts begin with creating a bag of unique words from the texts, words that will be used to establish the criteria the design of bag words a transformation of texts to numerical values made. These texts count the number of times that each phrase is repeated, thus creating a training matrix. With the data already pre-prospected, the training is performed. After data processing, the Random Forest algorithm had an accuracy of 84% used to predict future texts.

Once the analyzed algorithms are clarified, we can graphically (Figure 2) the selection processes of the individuals. We can appreciate more greatly the comprehension

of the article detailed here. From which we can say that to process the information, it is necessary to have a database of the information capture of the study.

It will help us to be able to determine the mental fatigue of the individuals and thus to be able to look for improvements in the production to help the workers in this subject.
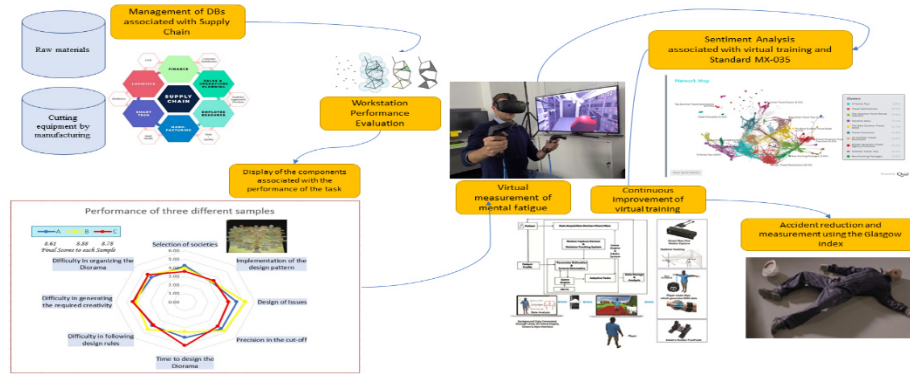
Fig. 2. Mental fatigue analysis scenario

4 Results

The Bayesian algorithm gave us a result in favor of the men. Due to the pressure to increase the number of parts, the male group continued to perform activities, making it more productive. Still, compared to the results presented in the female group, the quality is lower, and the concept of quality is prioritized, i.e., increasing production and minimizing delays. However, among the analysis subjects, the female group is more detailed than the male sample. The female group is only interested in mass production. Factors such as age, gender, and shifts also show more significant differences in job performance and mental fatigue.
.

NAÏVE BAYES
We have the results obtained by the Weka program from the analysis of the Naïve Bayes algorithm, which can be seen in figure 3.

Scheme: weka.classifiers.misc.InputMappedClassifier -I -trim -W weka.classifiers.bayes.NaiveBayes

Relation: mentalfatigue-weka.filters.unsupervised.attribute.StringToWordVector-R1-W1000-prune-rate-1.0-N0-stemmerweka.core.stemmers.NullStemmer-stopwords-handlerweka.core.stopwords.Null-M1-tokenizerweka.core.tokenizers.WordTokenizer -delimiters " \r\n\t.,;:\'\"()?!"

Instances: 33
Attributes: 47

Correctly Classified Instances	28	84.85%
Incorrectly Classified Instances	5	15.15%
Kappa statistic	0	
Mean absolute error	0.271	
Root mean squared error	0.3591	
Relative absolute error	100%	
Root relative squared error	100%	
Total Number of Instances	33	

=== Detailed Accuracy By Class ===

TP Rate	FP Rate	Precision	Recall	F-Measure	MCC	ROC Area	PRC Area	Class
0	0	?	0	?	?	0.5	0.152	f
1	1	0.848	1	0.918	?	0.5	0.848	m
0.848	0.848	?	0.848	?	?	0.5	0.743	

=== Confusion Matrix ===

a b <-- classified as	
0, 5		a = f
0, 28		b = m

Figure 3. Results of Naïve Bayes algorithm

MULTILAYER PERCEPTRON

The analysis of the multilayer perceptron shows us the result in the classes of the three work shifts, taking as the highest productivity in the first shift that this algorithm categorizes the values in production, leaving aside the other types analyzed in the article.

We can see the breakdown of the data inputs on the left side of Figure 4. There are three hidden layers of 5,10,20 neurons in the central part, and on the right side, we find the data output nodes. At the same time, we have the results obtained by the Weka program from the analysis of the multilayer perceptron, which is shown in figure 5.

Run information:
Scheme: weka.classifiers.misc.InputMappedClassifier -I -trim -W weka.classifiers.functions.MultilayerPerceptron -- -L 0.3 -M 0.2 -N 500 -V 0 -S 0 -E 20 -H a
Relation: mentalfatigue-weka.filters.unsupervised.attribute.StringToWordVector-R1-W1000-prune-rate-1.0-N0-stemmerweka.core.stemmers.NullStemmer-stopwords-handlerweka.core.stopwords.Null-M1-tokenizerweka.core.tokenizers.WordTokenizer -delimiters " \r\n\t.,;:\'\"()?!"
Instances: 33
Attributes: 47
=== Summary ===

Correctly Classified Instances	24	72.73%
Incorrectly Classified Instances	9	27.27%
Kappa statistic	0.5909	
Mean absolute error	0.1969	
Root mean squared error	0.3278	
Relative absolute error	44.30%	
Root relative squared error	69.54%	
Total Number of Instances	33	

=== Detailed Accuracy By Class ===

	TP Rate	FP Rate	Precision	Recall	F-Measure	MCC	ROC Area	PRC Area	Class
	0.818	0.136	0.75	0.818	0.783	0.668	0.942	0.928	first
	0.636	0.091	0.778	0.636	0.7	0.577	0.868	0.845	second
	0.727	0.182	0.667	0.727	0.696	0.535	0.921	0.856	third
Weighted Avg.	0.727	0.136	0.731	0.727	0.726	0.593	0.91	0.876	

=== Confusion Matrix ===

```
a b c  <-- classified as
9, 0, 2 | a = first
2, 7, 2 | b = second
1, 2, 8 | c = third
```

Figure 4. Results of Perceptron algorithm
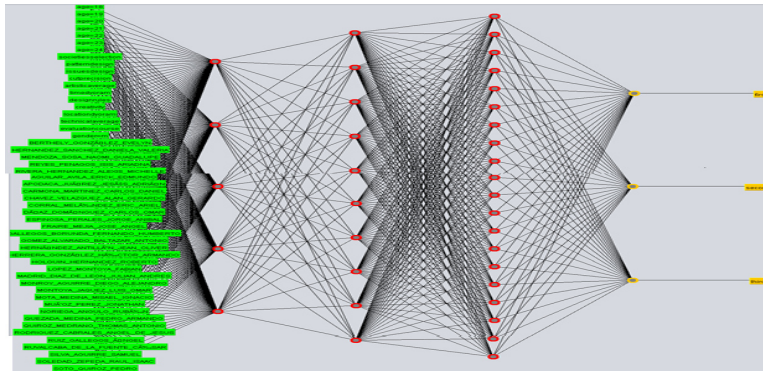
Figure 5. Neuronal network of mental fatigue

Random Forest

The Random Forest shows us 47 trees executed in the algorithm. We can obtain a result of instances classified in 93.94% evaluating the age class of the three different groups, showing significant differences in work performance in the mental fatigue of each worker. Mental fatigue is the highest efficiency found in the ages between 21 and 22 years old.

We can see in Figure 6 the run of the data produced by the Weka program using the Random forest algorithm.

=== Run information ===

Scheme:weka.classifiers.misc.InputMappedClassifier-I-trimWweka.classifiers.trees.RandomTree -- K 0 -M 1.0 -V 0.001 -S 1

Relation: mentalfatigue-weka.filters.unsupervised.attribute.StringToWordVector-R1-W1000-prune-rate-1.0-N0-stemmerweka.core.stemmers.NullStemmer-stopwords-handlerweka.core.stopwords.Null-M1-tokenizerweka.core.tokenizers.WordTokenizer -delimiters " \r\n\t.,;:\'\"()?!"

Instances: 33
Attributes: 47
Size of the tree : 47
=== Evaluation on test set ===
Time taken to test model on supplied test set: 0.01 seconds

= Stratified cross-validation =
= Summary =

Correctly Classified Instances	31	93.94%
Incorrectly Classified Instances	2	6.06%
Kappa statistic	0.9285	
Mean absolute error	0.0202	
Root mean squared error	0.1058	
Relative absolute error	8.31%	
Root relative squared error	30.37%	
Total Number of Instances	33	

=== Detailed Accuracy By Class ===

TP Rate	FP Rate	Precision	Recall	F-Measure	MCC	ROC Area	PRC Area	Class
1	0	1	1	1	1	1	1	18
0.8	0	1	0.8	0.889	0.879	0.993	0.943	19
1	0.037	0.857	1	0.923	0.909	0.984	0.952	20
1	0	1	1	1	1	1	1	21
1	0	1	1	1	1	1	1	22
0.8	0	1	0.8	0.889	0.879	0.996	0.967	23
1	0.036	0.833	1	0.909	0.896	0.996	0.967	24
Weighted Avg.	0.939	0.012	0.949	0.939	0.939	0.931	0.997	0.973

=== Confusion Matrix ===

a	b	c	d	e	f	g	<-- classified as
3	0	0	0	0	0	0	a = 18
0	4	1	0	0	0	0	b = 19
0	0	6	0	0	0	0	c = 20
0	0	0	3	0	0	0	d = 21
0	0	0	0	6	0	0	e = 22
0	0	0	0	0	4	1	f = 23
0	0	0	0	0	0	5	g = 24

Figure 6. Results of Random Forest

5   Discussion

This study used a qualitative design to examine psychosocial factors, work stress, and mental stress as applied to the automotive industry, focusing on a company engaged in the production of fabric cutting for car seats. Although this paper aims not to evaluate gender differentials, we emphasize a few critical gender issues that are relevant and valuable for mention. Compared to men, there were fewer female study participants involved in the work shifts analyzed. In the tailoring management value chain, women have the highest role, which shows that women tend to do more beautiful and efficient work. Some reasons, such as cultural and socio-cultural value systems, consider cleanliness and precision cutting as traditional female roles, which can improve production and thus realize the cutting function.

The occupational hazards with workers ' activities are minimized through the systematic use of personal protective equipment (PPE). Previous cutting and sewing

training courses can also minimize them to understand the process pattern to be followed. However, the committee members stated that their working conditions are terrible and the work pressure to finish the product on time is far from seeking better production quality. Hence, there are quality failures related to the pressure to achieve the target. The company has established daily production but has not received sufficient training in abatement measures and work-related practices and methods for reducing health hazards. These situations seem to indicate that they have limited skills to identify the psycho-social risks related to their work surroundings and implement safety and health precautions.

Conclusions

Risk management is one of the main activities of modern supply chain management. One of the main risks is operational risk, which is linked to the level of mental fatigue that operators can tolerate, as well as their wandering mind [9,10]. These risks are inherent to the daily activities of the company, perhaps operational risks do not have the degree of destructive risk, but without their consideration and management, they will significantly affect business results [10]. The flexibility of employee participation is relevant, because they are indispensable when performing activities to overcome changes in the demand and production of items, they are what makes them suitable for the production process to adjust to them [11].

The automotive workers who participated in the study faced risks related to mental health and reported unsafe behaviors related to the company's measures to ensure a good working environment. Workers are also aware of the implementation of standard production control procedures related to the management of fabric manufacturing. Still, the company does not comply with occupational health and safety standards regarding production quality.

The study presents three different results: the evaluations are age, gender, and work shift, wherein part of the gender clarifies that the most efficient was the male group. The concepts were evaluated with the Bayesian algorithm. Most of the data collected in the three assessed groups were of male origin since the female group was only 15% of the population analyzed. Although the result was given for the male group, it is necessary to understand the data analyzed where the female group presented better results in production quality.

On the side of the work shifts, it was found that the algorithm of neural networks or multilayer perceptron gave us favorable results. The first shift is more efficient than the other two analyzed. It is necessary to understand cultural impact since we had the same amount of personnel studied between the other two groups. When analyzing the three groups by their ages with the random forest algorithm, we found that the most effective ages for production were between 21 and 22 years of age, mixing genders and work shifts. The variation of ages is similar in the three groups analyzed.

Poor interpersonal relations between workers and their managers and the lack of social protection and job security are other problems that harm workers' social and mental health needs. Negative attitudes, perceptions, and stigmatization of workers by the community and lack of production standards lead to low job pressure and satisfaction. A tailored workplace policy is needed to provide counseling and psychosocial support in a social psychology company canteen and help employees improve work stress management. In addition, the company policy should comply with the standard Mexican NOM-035 on psychosocial risk factors, solve problems and solutions to avoid this impact in the workplace, especially among low-wage workers, which will seek to improve job satisfaction observed in this study.

References

1. NOM-035-STPS-2018, Occupational psychosocial risk factors � Identification, analysis and prevention. Mexlaws.com. https://www.mexlaws.com/STPS/NOM-035-STPS-2018-information.htm (2018). Accesed 23 Octuber 2021
2. De Croon E, Sluiter J, Kuijer PP The effect of office concepts on worker health and performance: a systematic review of the literature. Ergonomics (2005) 48(2):119–134
3. Seddigh A, Stenfors C, Berntsson E, Bååth R The association between office design and performance on demanding cognitive tasks. J Environ Psychol 42:172–181 CONFERENCE 2016, LNCS, vol. 9999, pp. 1–13. Springer, Heidelberg (2016).
4. Greenwood DC, Muir KR, Packham CJ, et al. Coronary heart disease: a review of the role of psychosocial stress and social support. J Public Health Med 1996;18:221–31.
5. Hemingway H, Marmot M. Evidence based cardiology: Psychosocial factors in the aetiology and prognosis of coronary heart disease: systematic review of prospective cohort studies. BMJ 1999;318:1460–7.
6. Harper S, Lynch J, Hsu WL, et al. Life course socioeconomic conditions and adult psychosocial functioning. Int J Epidemiol 2002;31:395–403.
7. Marmot MG. Bosma H, Hemingway H, et al. Contribution of job-control and other risk factors to social variations in coronary heart disease incidence. Lancet 1997;350:235–9.
8. Marmot MG. Improvement of social environment to improve health. Lancet 1998;351:57–60
9. Cuadra, R. Frequency of Mind-Wandering in a Sustained Attention to Response Task: A Cognitive Model of Distraction. (2020). Res. Comput. Sci., 149, 11-21.
10. Pastrana-Jaramillo, Carlos & Osorio, Juan. (2019). Operational Risk Management in a Retail Company. Research in Computing Science. 148. 57-66. 10.13053/rcs-148-4-6.
11. Díaz-Reza, José & García-Alcaraz, Jorge & Avelar, Liliana & Mendoza-Fong, José. (2020). The Role of Employees' Performance and External Knowledge Transfer on the Supply Chain Flexibility. 10.1007/978-3-030-26488-8_2.

Intelligent social forecast in the Olympic program of La Laguna: A multicultural perspective

Leonardo Nahle-Ortiz[1], Alberto Ochoa-Zezzatti[2], Gerardo Yañez-Betancourt[1]

[1]Ibero Torreón

[2]Juarez City University

Abstract

In this research, three multicriteria decisions (MCDM) analyses are applied using the TOPSIS (Technique for Order of Preference by Similarity to Ideal Solution) methodology in managing the Olympic program of La Laguna. The model is structured and conceptualized as an intelligent social forecast system and integrates KPI`s (Key Performance Indicator) such as PISA (*Programme for International Student Assessment)* test, cultural cohesion metrics, and Olympic medals as an output of the entire model and program. Multivariate statistical and other qualitative techniques such as structured modeling equation (SEM) and paradigms such as Cultural algorithm, social portfolio problem, and demographic data are used. The model is ennobled with social theories, and the concept of aleph places is presented and introduced. It is pointed out how the MCDM decisions integrate the intelligent support system within the intelligent component, with high potential for other artificial intelligence applications. Finally, as next steps, it is established that a data set with the profile and history of each medal winner along with a case study is necessary to establish several scenarios that will help model social capital processes. These qualitative methods must be addressed in the context of the Imaginary Institution of Society.

Keywords: MCDM, TOPSIS, Laguna Olympic Program, Cultural algorithms, socio-cultural-urban interfaces, social portfolio problem, and Aleph places.

1.- Introduction

A Smart City is characterized by being made up of different components, one of vital importance is the physical health of children and young people. "Divide and conquer", the Romans used to say. Today, with the change of historical chronotope already predicted by Hans Ulrich Gombrich[1] and potentiated by the great technological corporations in times of pandemic, the only alternative for citizens is to evolve and cities are the first place, cities are the battlefield where all these changes will take place. Equipping them with the requirements so citizens can succeed in this greater good is a critical task; soon *dive et impera* will be a thing of the past in any contemporary society. Move heavy artillery so that our social capital is superimposed on our groups, communities, and society; an alignment of capabilities that can be designed systematically, *Smart Cities* is the paradigm to adopt. [13] The sum of collective intelligence recognizing problems created by ourselves in the past and aspire to our full potential. Every instance a human subject integrates and incorporates the social structure; new hybrid processes and places where humans interact, new paradigms emerge, new strategies designed to influence society, evolve to a higher level, and reach the maximum human potential, Maximize the use of resources of our region, and build a new society. A way of projecting the cultural integration in La Laguna within the framework of a smart city.

Cultural Algorithms Cultural Algorithms (CA) [2] is a sub-discipline of evolutionary computation, whose knowledge component is called Belief Space, Fig. 1, in a certain group or population. Cultural algorithms were introduced by Reynolds [2]. Idealized approaches to cultural evolution by several scientists include the following: Edward B. Tylor was the first to introduce the term "culture" in his two books on primitive culture in 1881; he conceived culture as "A complex whole which includes knowledge, beliefs, art, morals, customs, and every other capacity and habit acquired by man as a member of society". Early approaches to the study of culture focused on the classification of cultures around the world into groups based on "adhesions" between cultural elements and/or components. In the 1960s, cultural ecology emerged as a discipline concerned with the nature of interactions between the cultural system and its environment. The 1970s saw a new emphasis on how culture shaped the flow of information in a system, a generalization of the cultural ecology perspective. Geertz in 1973 in his book, The Interpretation of Cultures, exposes culture as the fabric of meaning in terms of which human beings interpret their experience and orient their actions. William H. Durham in 1990 wrote the article titled, Advances in evolutionary Culture Theory said "Culture is a shared ideological phenomenon (values, ideas, beliefs, etc.)" [3]. A Cultural Algorithm can be conceptualized by the following Pseudocode in Figure 1:
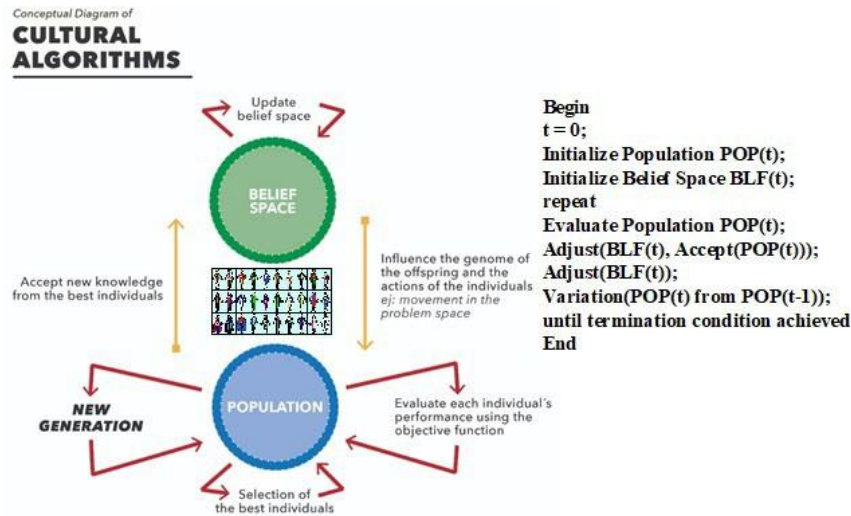
Fig. 1. Conceptual Diagram of Cultural Algorithms.

The introduction of cultural algorithms as an initial concept in this article has a purpose; it is the representation of the macro system in which we would be making different cultural algorithms for the creation of a Smart City in this occasion the Cultural Algorithm, Olympic Program of La Laguna (POLL), is one of them; more cultural algorithms or modules can be incorporated; so to speak; this is how one by one we can add different algorithms that contributes to the conceptualization of the Smart City. So then by refining and improving other existing algorithms which would be designed to maximize the

contribution to the Smart City. In Torreón the concept is not new, a case of success locality on which we elaborate our Cultural Algorithm, the POLL. Yohan Uribe Jimenez, deputy editorial director of the local newspaper; *"El Siglo de Torreón"* , recently rescued a successful experience, in his conference *Architecture against violence*. This is the case of the Cultural and Sports Complex "Antigua Jabonera La Unión" shown in Fig. 2, located between the colonias la Primera and Segunda Rinconada, in the west of the city of Torreón, an underdeveloped urban area. According to the IMPLAN webpage, this endeavor had a positive impact on the population of this sector, previously affected by crime. The project, linked to the concept of urban recycling[1]; Yohan argues the project resulted in a success case study, where the mix of architecture and sports is a clear case of a successful cultural algorithm in an already existing old and ruined property. Rescued from gangs, embellished with architecture and of course along equipment and furniture, this industrial vestige, is then transformed and can attract children and young people associated with gangs. Practically we could be saying that we are scaling up a success story to the whole La Laguna territory:

(A)   (B)

Fig. 2. Facilities of the cultural and sports complex. Antigua Jabonera La Unión:

(A) Blueprints of the project for the recovery of the physical space.
(B) Front of the property.

2.- Problem scope and description.

Based on the datasets associated with the most recent information from CONADE's 2019 and 2021 Olympics; and other primary sources of information, we can appreciate a great difference in the number of medals between in our cities from both overall state results, 36 Medals in Durango and 112 medals in Coahuila, corresponding for Torreón: 9; Gómez Palacio: 0; Lerdo: 0. Against the state capitals Saltillo 77 medals and Durango 44 medals and corroborated with local sports organizations and institutions. It can be said that Coahuila's state delegation excelled during the CONADE (National Commission on Physical Culture and Sport) 2021 national Olympiad. Coahuila doubled the participation of athletes compared to the last edition. The state delegation won 112 total medals, a historic achievement for our state sport, of which35 were gold, 25 silver, and 52 bronze. Coahuila is positioned in 9th place in the national medal ranking in 2019 it was in 17th place. Now, the distribution clearly is not congruent, clearly an unbalanced situation. We already have identified critical variables as unequal dispersion of economic resources from CONADE and SEP (National Ministry of Public Education),by the head states of Coahuila and Durango.

---

[1] Rescuing antique and old government buildings or properties and incorporating into the urban support network

A good strategy was implemented in Coahuila since the playoffs of some sports were held locally, a successful strategy that brings more sports closer to our community indeed; this resulted on a tipping point triggered by local participation, thereby contributing to more medals in the region: 3X3 basketball, fronton (Trinquete and 30 m), rugby 7, baseball, racquetball, although in team sports, we hardly aspire to Olympic medals, except softball that there was a preferential political decision in Saltillo to favor their team. National soccer and field hockey qualifiers were held in Durango. It should be noted that 2020 is a very atypical year because of COVID-19, and it is important to point out that in 2021 the national budget for CONADE was reduced, resulting in a decrease in the budget for all of Mexico. From 2 thousand 676.5 million pesos for the Olympic year, a reduction of 107.5 million pesos compared to 2020. Since there were no competitions because of the COVID-19 pandemic. In a recent interview with the deputy director of the Municipal Sports Institute (of Gomez Palacio, Durango) he commented that in the state of Durango there were no economic resources from the government State Sports Institute, specifically for operation and day to day spending, triggering the discrimination process against La Laguna. As a result of all these situations, there is low participation in the National Olympiad. Findings during the interviews very interesting facts and situations emerge:

- During the National Games CONADE 2021, Coahuila doubled the participation of athletes compared to the last edition of the National Olympics (previous name of these games).
- Coahuila achieved 112 medals in total, a historic achievement for our sport, of which 35 were gold, 25 silver, and 52 bronze.
- Coahuila is positioned in 9th place in the national medal standings

The objective of the *Physical Culture and Sports Program* in the Federal Expenditure Budget is to benefit the Mexican population aged 6 years and older, through the Physical Culture, Sports and High-Performance strategies implemented by CONADE, without discrimination and in coordination with the Physical Culture and sports bodies, national sports associations, and other related organizations. As we mentioned before, it is important to highlight that in 2021 national budget for CONADE will be reduced, representing a total decrease of 107.5 million pesos, In a recent interview with Diego de la Garza Adriano, subdirector of administration and sports infrastructure in Gómez Palacio, and Lic. Moisés Arce Daher, director of the Instituto Municipal del Deporte in Torreón, both commented there is no hope of receiving economic support from either states Durango, and Coahuila, it's almost a custom and tradition in our region.

Demography for the POLL A fundamental aspect of our model is the forecast is to incorporate the issue of demographics; to ensure a good capacity it is necessary to incorporate demographic data; this forecast is based only on the populations of Torreón, Gomez Palacio, and Lerdo; data is based on the last count conducted by INEGI survey in 2020, Fig. 3, gives us a good estimate and allows us to make extrapolations the POLL capacity in the following years.

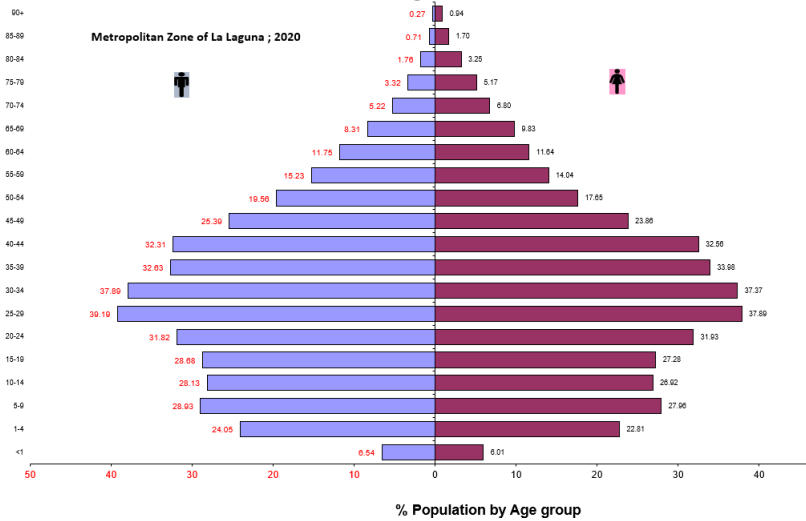It is concluded that La Lagunarequires capacity for 430,500 habitants in the next 5 years on a yearly basis.

Fig. 3. Demographic data for Metropolitan Zone of
La Laguna (Torreón, Gómez Palacio and Lerdo).

Metropolizitation. The metropolitan perspective for the integral development of La Laguna submerged in an interstate metropolitan area, since its cities are in 2 states: Durango and Coahuila. Metropolizitation is an obligatory concept in many aspects of the social and urban processes within the Smart City [5] Laguna, this process gives a weak light on the horizon where there is fog and the POLL a solid structure in which citizens would bet and grow as individual and community, underpinned by the Olympic values: discipline, excellence, friendship. interests that 15 cities or municipalities represent important challenges, accelerating conurbation processes, identifying interest groups, and exploiting the combined capacity between municipalities. Our metropolis Torreón, Gómez, Lerdo, Matamoros and Francisco y Madero is the 10th largest metropolitan area of La Laguna out of others metropolitan areas. The POLL and its capability to reach this entire region with services. Nevertheless, the law of metropolitan interests are environment, water, security and justice, community, and metropolitan governance it is set up; other interests undermine our metropolizitation processes. Once again, these interests divide and tear us apart as tribes, groups, and society and as a result, a divided society that also leads to a brain drain. If a city is not capable of retaining its talents, it is a city where there is no quality, and La Laguna phenomena like these emerge. In a survey of experts in metropolizitation, we ask for the qualified opinions of 10 experts, allowing us to detect the metropolizitation of social processes is not even 25% advanced. In the specific case in sports: a metropolitan tournament was organized before the Covid- 19 crisis in 2019 and attendance was low. The POLL has the potential to provide impetus and momentum to all these processes. It is draw to our attention in our research identifying the scope of this metropolizitation almost identical in spirit and issues to the Smart City initiative [15].

Social capital. The formation of social capital is created through cultural practices and social exchanges based on values as is possible to be seen Figure 4 [9]; there are many forms to model social capital many based on tactical strategies of social capital accumulation. But when projected to the public at Olympic events, enhanced by the mass media, it is the interconnection between the three key Olympic values: respect, friendship and excellence, and society these values are emulated to the crowd of people participating during the event; the study of Olympic social capital has generated many theoretical inventories in the academic literature. Already as a sub-discipline, the concept of Olympic social capital creates a network of relationships; the formation of this network interconnects all the actors involved, whether as athletes, organizers, live attendees, spectators, or even radio listeners[6].

Fig. 4. A sample of children practice golf in La Laguna.

The Olympic concept and its core product the Olympic Games, benefit from the values of Olympism, which is unique in the world of sport and fosters the creation of social capital[6]. The simultaneous experience perception and cultural practice of Olympic values, transform the individual on a collective level and thus form a binding and deploying social capital [7], extensive global media coverage and other complements links social capital within the economic and political sphere of the context [8].

Towards plausibility ad hoc model for La Laguna. Social and professional interactions can also cause the erosion of Olympic social capital. In this context, it is critical that the Olympic message effectively reaches the largest Olympic stakeholder group in a global audience, everything is interconnected. Live viewers go through a cycle of simultaneously shared experiences, resulting in an episodic memory of Olympic values that is stronger and more sustainable in the collective memory. This would also be the case for the POLL; Complexity exists in this communication process. The task becomes complicated, but a social issue of entrepreneurship aligned as well with the Smart City it's the recipe to ignite, this powerful process. Integrating multivariate models in real-time on web, with GPS capability and even scenarios where IoT instruments and devices can interact with the model. Recalling the Cultural Algorithms (CA) section of this paper, the Macro perspective of the CA helps us ground the model and put a baseline on society. Many cause - effect variables can stimulate the Olympic social capital processes [9]; but this can only be testable not only by implementing the total model, but several pilots can also allow us to check results and experiments, and then extrapolate. It is the iteration of the CA that allows us to present social capital as an element to be incorporated in the **Belief Space**; and gradually develop a new social worldview derived from the POLL.

The infrastructure it's a key variable that allows us to accumulate social capital; this infrastructure will have to be competitive according to global standards; this triggers the accumulation of social capital and incorporating it into the worldview of a smart city. It is the accumulation of several strategies that will generate what is called "A bathtub metaphor dynamics"; the iteration of this process generates the adequate competencies and "capability build-up" helping us develop deliver the Belief space and / or "Olympic game capability" [7] within the smart city, one more feature to reach our maximum potential at La Laguna. **PISA Test.** PISA is the acronym for the *Programme for International Student Assessment*. It is an effort of the OECD (Organization for Economic Cooperation and Development), whose purpose is to evaluate the capacity and training of students when they reach the end of compulsory education, at the age of 15. This is a population that is about to starttheir working life or begin education at the high school stage. The PISA Test Program is conceptualized as a tool to offer abundant and detailed intelligence that will allow the adoption of decisions and public policies on a critical path to increase the educational levels or ranking of the countries that are members of the OECD. Allowing us to benchmark globally. The areas of reading, mathematics, and scientific competence are evaluated. There is an emphasis on the mastery of processed, the understanding of concepts, and the ability to act and function in real situations in each domain. A proxy for assessing social capital can be use this indicator to establish a baseline, if the entire population is processed through the POLL, it should increase the PISA Test as well; maybe in the future can be another variable to assess within the program or even develop a CA for education, another socio-cultural-urban interface for the Smart City.

3.- Programa Olímpico de La Laguna (POLL)

Fig. 5. Brand of the Olympic program of La laguna (POLL).

"In the modern world, full of powerful possibilities and threatened at the same time by dangerous decadences. Olympism can constitute a school of moral nobility and integrity as well as of physical strength and energies; but this will require as a condition that you raise and maintain unceasingly your concept of honor and sporting disinterest at the height of your muscular impulse", see Fig. 5. These words were written by Pierre de Coubertin, pedagogue, and historian, reflect the essence and justify the creation of the Olympic Program of La Laguna (POLL), the social construct that we are trying to put together that can fuel the people of La Laguna beyond our actual potential to Torreón, Gomez, and Lerdo and consequently to all La Laguna2. Agela Saini author of Superior the new science of race says: ".. After all race is a social construct, not a biological trait. That's the scientific consensus. So why do many still doubt it?.." strong words and old ones too , but she refers to the future as well. Table 1 are the elements of the Olympic program of La Laguna.

Table 1 Elements of the Olympic Program (POLL).

Elements of the Olympic Program (POLL)
Access to the Olympic Program
Coach and Athlete Training via the Web
Aleph Infrastructure or Smart City Hotspots
Assignment of Shadow Organisms
Access to Knowledge Base
Economic Support for Finalists
Associated costs to qualify

It is in the management of this social construct [8] and its prognosis where we theorize, design and build a model and system of support for intelligent decision making in the Olympic Program of La Laguna, in figure 6 [9].

Fig. 6. Components of POLL involving all Community.

Operationalization of the POLL As we had previously established, the operationalization of the POLL starts with a supra-systemic model called Cultural Algorithms; in it, we will be able to perform many iterations, it is the tenacity of the team and athlete that gives life to the program, we will be able to see a flow of a percentage % of the population, and be able to monitor its performance and thus the POLL in general. The POLL seeks to achieve certain results for the region KPI`s categories.

---

2 What is Olympism (https://olympians.org/woa/olympism/?langid=3)

Table 2 KPI`s Database Categories.

KPI's Databases Categories
User Profile
Athlete recruitment and retention (Track Record)
Geolocation
Visualization
Profitability
Users, partners, and Collaborators
Social Capital Creation
Serviceability

The categories of KPI`s, help monitor the processes; but the POLL's main success will be measured in terms of benefits in medals, the latent variable. Program management includes management of projects for achieving capability in the three areas Socialization, Sports, Infrastructure, and Connectivity. POLL favors more accurate management in central or local government, including providing a better service to the community. A Program manager who accounts to the program sponsor (or board). Runner up orchestrators for the program could be organizations such as La Comunidad de Instituciones de Educación Superior de La Laguna (CIESLAG) and Asociación Deportiva Universitaria de La Laguna (ADUL). The program must react to changes in strategy and changes in the environment in La Laguna. But above all exploring the best options to integrate the POLL: Sports (materials, training, and knowledge), infrastructure and connectivity, and finally Socialization are some of the final and critical deliverables of the Decision Support System (DSS) of the POLL to yield a better outcome.

4.- Description of the Decision support system (DSS). Fig. 7. The key to the system is the consultation of interdisciplinary experts in both sport and sport program management such as doctors, team members, coaches, medal winners, etc. This system begins to be nourished with the experience of experts in the issues addressed by the MCDM decisions and each MCDM draws on experts in the criteria that each MCDM requirements and demands. The following block diagram illustrates the essence of the DSS, and information in each block addresses addressing the function the algorithms need to model and implement. The DSS plays a critical role and in the multicriteria decision method (MCDM), more than an obscure method, it is a simple method in the model to classify the intelligence for the decision to be made. The three MCDM methods proposed to build the initial DSS have an easy and accessible weight calculation. For this we use interviews and weighting methods. By carefully selected method and coefficients used; the MCDM should provide the basis for a very good forecast. Emphasis in the importance of choosing the correct method for a given multicriteria decision support model and DSS. Input data by experts and then comparing them by a conglomerate experience the weighted data is generated, for the POLL ensuring a structured method for the elicitation of weights incorporated in the model. Furthermore, providing different weighting

methods, and techniques with the possibility to compare within coaches and, experts of specialized knowledge, may increase interest among the actors of the POLL as well. Awareness and a competitive situation emerge by establishing a track record, benchmarks provide the basis to stay competitive. Other weighting methods, objective, subjective or hybrid, can be used in future experimentation. A good practice is to compare the results of objective methods with expert assessment. Additionally, more comparative methods can be applied and considered enabling a broader spectrum and support structure for the analysis.
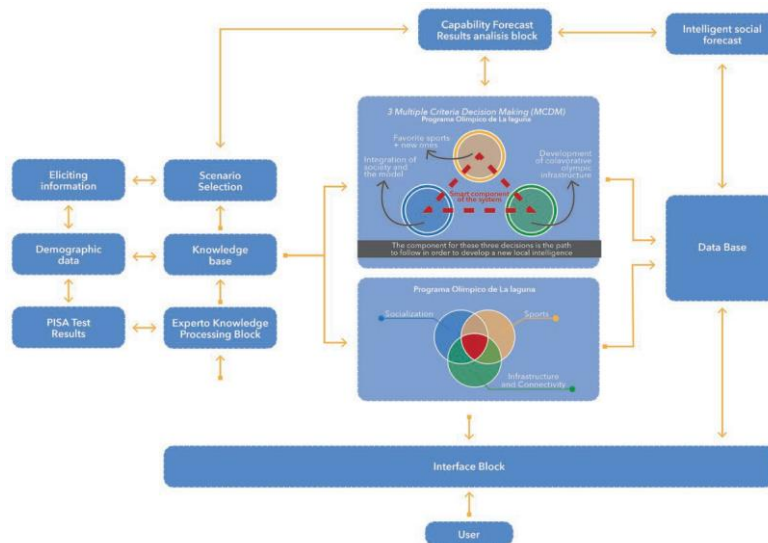

Fig. 7. Intelligent multicriteria analysis applied to POLL Block Model.

The Intelligent System Component of the database is conceptualized in three categories Fig. 8. which are the universes of the MCDMs: Favorite Sports, Socialization, Infrastructure Development.
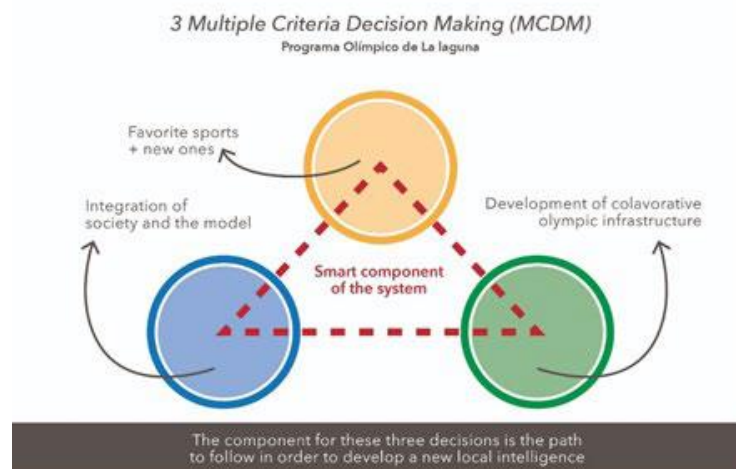

Fig. 8. "3 Multiple Criteria Decision Making (MCDM)".

12

Favorite Sports. A sample of 5 sports in Fig. 9. was generated out from the 55 sports that make up the CONADE National Olympiad. This small selection is made according to regional interests, medals won historically and new sports emerging in the international Olympiads. These are the growth areas of the POLL.

New Sport	spaces	Gender	Social status	Fun	Climate	Increase Health	Cost-Benefit	Associated with Cultural Identity	Socialization	Relevance to	Scholar practice
Skating	8	m-.50, f-.37	0.498	0.914	0.774	0.715	0.387	0.815	0.515	0.769	0.066
Surf	2	m- 40, f- 30	0.857	0.714	0.851	0.879	0.568	0.318	0.343	0.646	0.642
Sport Climbing	7	m-50, f-.40	0.617	0.658	0.385	0.712	0.514	0.904	0.81	0.563	0.145
Break Dance	11	m-48, f-.43	0.275	0.637	0.416	0.748	0.885	0.768	0.071	0.897	0.948
Ciclismo BMX	3	m-44, f-.26	0.391	0.939	0.181	0.455	0.889	0.441	0.207	0.656	0.679

Fig. 9. Sports Sample for the POLL.

Socialization. A network of vigilante's is required to promote and support the socialization of the project in different areas. Twenty-four civil society organizations identified, would be the support network for the POLL; it is important to select the *most prestigious, most related to the project and, solid* in La Laguna. Among the roles that these organizations would play in the POLL would be the supervisor, socialization of the results, campaign network. But it is above all the communication of what happens in POLL to society and its management a sense of reality.

Infrastructure Development. Coined as Aleph place or Smart City Hot spots. Intelligence developed by the POLL in these places; this intelligence must be identifiedthrough different approaches and epistemes along with social processes.

5.- Models
The following procedure used to calculate the MCDM decisions solved by TOPSIS method [4]
1) Elicitation of weight coefficients in categories and requirements.
2) Matrix normalization
3) Calculation of Euclidean distance generating result or ranking based on the Mahalanobis distance [9]

For the calculations between the distances of latitude and longitude, on the second and third MCDM, we use the haversine formula which determines the distance between two points on a sphere given their longitudes and latitudes, shown in equation 1.

$$d = 2r\ arsin\left(\sqrt{Sin^2\left(\frac{\emptyset_2-\emptyset_1}{2}\right) + cos(\emptyset_1)cos(\emptyset_2)sin^2\left(\frac{\gamma_2-\gamma_1}{2}\right)}\right) \qquad (1)$$

6.- Aleph Places[3] or Smart City Hotspots are identified, adapted and intercon-nected The Aleph places are the infrastructure where sports activities will take place. Incorporating the Aleph places into society, aligning them,

---

[3] Based on Borges' short story; recovering the idea that where there is Aleph, it becomes a cosmic place that makes us find sense and meaning in our lives.

and the evolution into true sports complexes and cultural centers can coexist, integrating Including the new runner up sports such as Skating, Gotcha and Kendo among others Fig. 14. Embellished with architecture and ornamental trees. In these places where we would also generate the intelligence required to find meaning in the lives of our current and future youth. Already with a database with possibilities and opportunities between clubs, public and private universities, sports units, can be also a point of interconnection, in here our young people will have strong foundations of our society. Equipped with a children's library, daycare center, outdoor theater, exhibition halls, and workshops; with spaces for pets; free Wifi, cafeteria, and if space permits, community markets that promote fair trade; these cultural centers would be spaces designed for the beginning of a change. All La Laguna would be converted into a true interconnected Olympic Village. For example, the issue of installed capacity at Aleph Places, see Fig. 10, is a critical issue to consider and is the MCDM and fundamental aspect of the POLL. According to a preliminary analysis of the existing infrastructure, there are up to 77 potential locations Figure 11 is an example; each place its analyzed and match with sports that can be adapted providing sports services in the Laguna metropolitan area.

Fig. 10. Distribution of collaborative Aleph spaces for sports in La Laguna, potential Aleph Places.
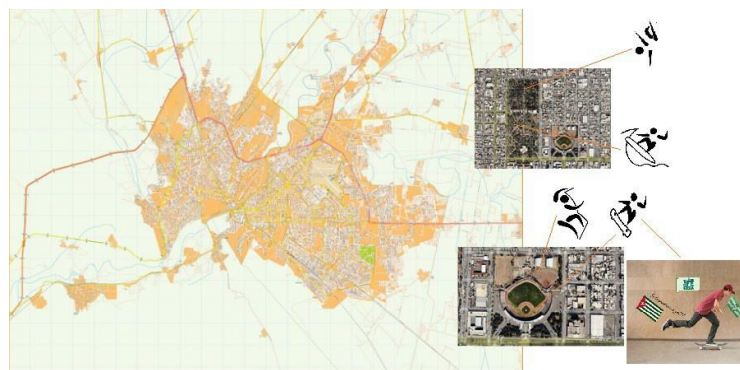

Fig. 11. Survey visits and budgeting process and prioritization would select the most viable and optimal space to influence the paradigm shift to a Smart City in La Laguna, four new Olympic sports were considered.

7.- Structural Equation Modeling (SEM)

SEM encompasses an entire family of models [10]. The intelligent social forecast of the POLL seeks to model medals, that is the latent variable. But before that happens our youth would have to work within milestones of the program that makes them get there, Fig. 12 is a model related to the research on the POLL. We are convinced that performance sports, socialization and adequate capability will deploy the latent variables, many medals. Pilots can be run, but the real information to increase social capital would be practiced, in the aleph places.
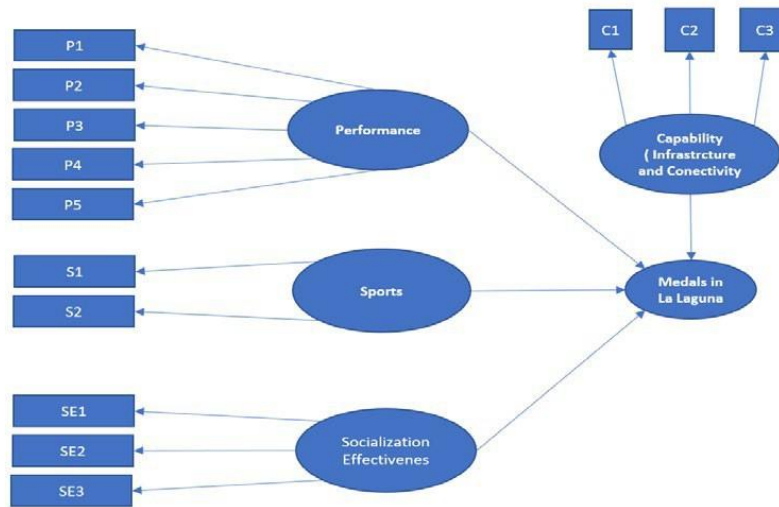

Fig. 12. Structural equation associated with the improved practice of sports in the POLL.

8.- Future Experiments

Mapping the Social Imaginary is a way to experiment within these algorithms, social theories provide an uncounted universe of situations and generate other applications for the forecast, institutions are not given once and for all, on the contrary, they are processes, imaginary interpretation compose them and require discourses, their practices, and rituals, all of these are forces in constant tension are put into play. The sum these institutions their processes, practices, rituals, and any force that influence the system under scrutiny should be mapped and found and used of Smart City Components, Fig. 13, these enablers coined as socio-cultural-urban interfaces would increase our reality to a new sense of citizenship approximation for Smart City.

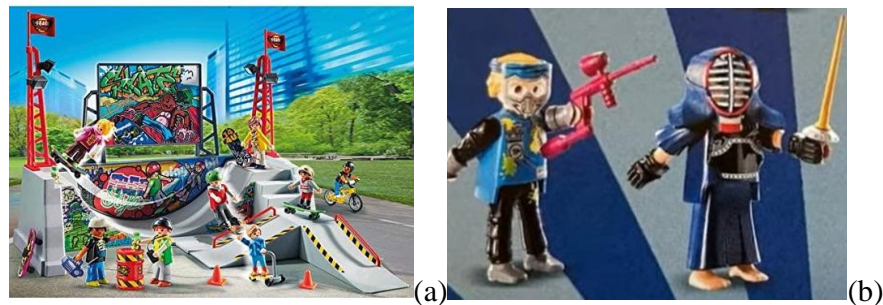
Fig. 13. Components in a Smart City.

Fig. 14. New Sports in the Olympics:
(a) Skating
(b) Gotcha and Kendo.

9.-Next Steps to build a correct POLL for "La Laguna"

First, refine series and increase model variables, then incorporate Rational Choice paradigm and other methodologies. Eventually, we will have to generate a business case and rollout for program advancement. Achieve socialization effectiveness in a network influence analysis and by using the CIGEL system; CIGEL stands for *Centro de Información Georreferenciada de la Región Lagunera* and incorporate new paradigms the POLL to have a geographic disaggregation, data analysis, and data mining, elements that help us integrate strategies to yield better results. Programs and project management will be the body of development of the POLL along with the communications process, which can lead to smart communication strategies to helpus build community and populate the POLL. The refinement and validation of the demographic series will help establish standards for budgets for the operation of the program. The survey each alternative must be done to generate and validate a budget; the evolution of a Network of Aleph Places will take the POLL to higher standards along with society [13].

10.- Result discussions

When we start to run the three MCDM decisions in their mathematical models we can observe the following: The most economical sport for access to the Olympics is Chess, this is derived from the ranking method used. There is no adequate infrastructure for the training of some sports such as Sport Climbing; there is only one gym that has a wall with adequate gear and equipment for the practice pf the sport. The year 2020 where there was no Olympics by Covid 19 pandemic and would be an absence of information for the forecast. The results of 2021 from the National Olympiad show a breakthrough in the overall number of medals, this should be attributed to an awakening of society to a new post-pandemic paradigm shift in society. There is an important number of medals between state capital Saltillo 77 medals and non-capital cities Torreón, 9 medals; this is not due to the anthropometric characteristics of the athletes but because of the economic resources the government deposits in its city capital for the use and practice of sports for the National Olympiad, this is verified in various interviews. Sixty-eight units or aleph places candidates already identified in the possible network in La Laguna this constitutes an opportunity for the creation of the POLL [14].

11.- Conclusions and future research

There is no competitive spirit in sports at La Laguna; this spirit is not promoted in the local schools and universities; sports are only promoted for health issues and a way to influence integral education. It is necessary to restructure the economic resources associated with the promotion of sports in La Laguna. Recent cases of Corruption4 in CONADE have detected fraudulent practices in amounts of $70 million of pesos; imagine all the athletes that can be potentialized by these economic resources. Another major problem detected in La Laguna is the duplication of athletes in local vs. state associations; the informatic system of CONADE is simply oriented to meet

state demands and not interstate interests as in the case of La Laguna. According to the current legal framework, there must be sports associations to trigger and generate interest in the practice of sport. Imagine 55 Olympic Sports associations and 32 states a total of 1760; that brings complexity to the ecosystem and a tangled situation that promotes corruption. Smart infrastructure in Aleph Places is a key component of smart cities. Sentimental analysis is a useful tool that is planned to be used in the Aleph places so that we can incorporate more intelligence into the forecast. Corruption is a factor that at the end of the day undermines the economic capacity of CONADE. New methods of resource dispersion and control must be incorporated into the federal public administration. Although there are three MCDM decisions, the information gathered to establish the MCDM decisions serves to generate future Artificial Intelligence applications. Design Thinking tools can be implemented for each athlete, discipline, or even tournament to achieve better performance and yield of the POLL. Ethnographic research can lead us to learn the success stories and gives us insight on those key issues governing the social capital creation these studies can be applied to medal holders so it can generate a model we can all relate to and lead younger folks to that success path[13].

---

4 https://wradio.com.mx/radio/2021/10/13/nacional/1634157538_368019.html

References

[1]   Ulrich Gumbrecht, Hans. El espíritu del mundo en Silicon Valley: Vivir y pensar el fu-turo DEUSTO (2020)

[2]   Reynolds, R. (2020). Cultural Algorithms: Tools to Model Complex Dynamic SocialSystems; December 2020 Wiley-IEEE Press

[3]   Palazzolo, T.J.The Cultural Algorithm Toolkit System. (2020).

[4]   Biernat, E., Nałęcz, H., Skrok, Ł., & Majcherek, D. TOPSIS for mobile based group andpersonal decision support system. (2020).

[5]   Bokolo, Anthony Jr. A case-based reasoning recommender system for sustainable smart city development. AI Soc. 36(1): 159-183 (2021)

[6]   Prüschenk, N., & Kurscheidt, M. (2020). Towards a Model of Olympic Social Capital:Theory and Early Evidence.

[7]   Prüschenk, N. (2020). Social Capital Creation Through Olympic Games - TheoreticalModelling and Evidence on Olympic Values.

[8]   Forsell, T., Tower, J., & Polman, R.C. (2018). Development of a Scale to MeasureSocial Capital in Recreation and Sport Clubs. Leisure Sciences.

[9]   Lee, S.P., Cornwell, T.B., & Babiak, K. (2012). Developing an Instrument to Measure theSocial Impact of Sport: Social Capital, Collective Identities, Health Literacy, Well-Being and Human Capital. Journal of Sport Management.

[10]   Junzo Watada, Masato Takagi, Jaeseok ChoiFuzzy Multivariant Analysis.(2004).

[11]   Burt, R.S.Applying data driven decision making to rank vocational and educational

training programs with TOPSIS. Decis. Support Syst., 142, 113470. (2000).

[12]   The Network Structure of Social Capital. Research in Organizational Behavior.

[13]   Sánchez Ramos, Inmaculada TESIS DOCTORAL Las "Smart Cities": Un nuevo paradigma. Aspectos Éticos.

[14]   Biernat, E., Nałęcz, H., Skrok, Ł., & Majcherek, D. (2020). Do Sports Clubs Contribute to the Accumulation of Regional Social Capital? International Journal of Environmental Research and PublicHealth.

[15]   Ramírez Hernández, Joselyne.Procesos e instancias de Gobernanza Metropolitana como respuesta al fenómeno de Metropolización en México. 2019. SEDATU.

Early Detection of Aortic Stenosis for the Prevention of Heart Failure in High-Risk Population using Whale Optimization Algorithm

Elda Betsabé Pérez Martínez[1], David Luviano Cruz[2], Soledad Vianey Torres Argüelles[3], Carlos Alberto Ochoa Ortiz Zezzatti[4]

[1] Universidad Autónoma de Ciudad Juárez, Doctorado en Tecnología, Cd. Juárez, Chihuahua, México

ebetsypm87@gmail.com,
david.luviano@uacj.mx,vianey.torres@uacj.mx,
alberto.ochoa@uacj.mx

Abstract. Currently, the pace of life of people in a Smart City has been incrementally affected due to several factors such as stress and risk diseases, including hypertension, diabetes, and even SARS. COVID'19 pandemic with a future prognostic of 7,87 million deaths to the middle of 2022- that leads to cardiovascular diseases and conduct to a heart attack, it has been observed that in Mexico it is recurrent from the range age near of 45 and one of the most common heart diseases is aortic stenosis and can reach be fatal if it is not detected in time. In practice, the echocardiogram is the fastest means to detect abnormalities anatomically and physiologically in real-time. However, the interpretation can be affected by the image quality. Therefore, there are techniques to improve noise for image processing and, where appropriate, separate the regions of interest. This is known as segmentation. In this research, a model inspired by artificial intelligence for diagnosis is proposed, the model uses Convolutional Neural Networks (CNN) as a deep learning technique for classifying images of Aortic Stenosis, and an innovative metaheuristic named Whale Optimization Algorithm (WOA) is implemented to select the most relevant segmentation feature of the Aortic echocardiographic view. The results show promising performance for the diagnosis.

Keywords: Whale Optimization Algorithm, Image Segmentation, Convolutional Neural Networks.

1. Introduction

Cardiovascular diseases are the leading cause of death globally and it is estimated that by 2030 the mortality rate will double, however, the statistics have changed due to the SARS variant and the current COVID 19 pandemic, the future forecast for 2022 is 7.87 million deaths. It has been recorded that this disease causes damage to the heart, even in patients who had not had any previous heart disease, causing heart failures that damage internal structures to cause a heart attack [1,2].

One of the main cardiovascular diseases is Aortic Stenosis that occurs in advanced age in adults and predominates more in the male gender, since it is presented by the narrowing of the valve or accumulations of calcium known as stenosis, also can be genetic conditions or in patients who have had a history of rheumatic fever, hypercalcemia or risk factors such as smoking, cholesterol, diabetes, hypertension among others. Once severe aortic stenosis occurs, the survival rate is only 50% at 2 years and 20% at 5 years without an aortic valve replacement, as long as the patient presents symptoms as it can go unnoticed for years until the first symptoms such as chest pains, shortness of breath and fainting [3]. That is why one of the devices of interest in the clinical practice to detect aortic stenosis is the echocardiogram since it does not represent a danger to the patient and is able to show images in real time of the physiology and anatomy of the heart, however, it is essential the detection and interpretation of the specialist so sometimes the quality of the image may be not optimal or the interpretation requires of time for detection and there are usually cardiopathies that go against time.

For the interpretation, detection and diagnosis in medical images, the processing of medical images allows us to determine the characteristics of the images obtained by the echocardiogram obtained from the different views, so segmentation is a key component in image processing to isolate physiological and biological structures of interest. Therefore, in this work the segmentation of the medical image is the fundamental part to obtain the main parameters of Aortic Stenosis and facilitate its interpretation. One of the most widely used applications of Artificial Intelligence is Deep Learning where Convolutional Neural Networks aids to classify, the idea of this architecture is to achieve a learning model that is capable of learning to filter the most relevant characteristics of an image. Likewise, metaheuristic algorithms, which are stochastic search algorithms use heuristics for any problem to accelerate convergences to nearby solutions in this case the main characteristic of the image segmentation allowing precision in the detection of Aortic Stenosis.

2.   Related Works

In a review of the literature associated with metaheuristics, it was determined that there are various algorithms that are focused on solving multi-combinatorial and multi-restrictive problems associated with the resolution and identification of possible plausible solutions that involve a set of longitudinal variables [4].

The parameter optimization study and evaluation metrics are useful for image segmentation. Within the works, different heuristics and metaheuristics have been implemented that have been applied to grayscale images that an echocardiogram gives us, for this type of images the use of the Particle Swarm (PSO) optimization algorithm or the optimization algorithm was found based on biogeography (BBO) with optimal results for segmentation problems and provide faster convergence with relatively less processing time. In recent studies according to Table 1. Multilevel segmentation to determine the optimal threshold values to segment a set of images using the Otsu method, diffuse entropy and Kapur's entropy as a fitness function has been favorable with the Whale Optimization Algorithm (WOA) [5]. Other segmentation techniques such as edge detection or Fuzzy C Means clustering or Support Vector Machine, simultaneously show an improvement in finding the local optimum and a higher convergence speed [6-10]. This algorithm is used even in others important applications as a parameter estimation of photovoltaic cells using an improved chaotic WOA [9].

Author	Year	Paper	Segmentation Technique
Aziz Abd El et al. [6]	2018	Multi-objective Whale Optimization algorithm for Multilevel Thresholding Segmentation	Multilevel thresholding
Nasiri et al. [7]	2018	A whale optimization algorithm (WOA) approach for clustering	Clustering
Vijh et al. [8]	2020	An intelligent lung tumor diagnosis system using whale optimization algorithm and support vector machine	Support Vector Machine Kernel
Fang et al. [9]	2021	Automatic breast cancer detection based on optimized neural network using whale optimization algorithm	Edge detection
Tongbram et al. [10]	2021	A novel image segmentation approach using FCM and whale optimization algorithm	Fuzzy C Means Clustering

Table1. Comparative studies with WOA algorithm in medical images.

3. Exploratory approach

In this section, the concepts used to image segmentation like convolutional neuronal networks, whale optimization algorithm, encircling prey, bubble-net attacking model, search for prey and WOA algorithm, that will be used for this work are analyzed.

3.1 Image segmentation

Image segmentation is a digital image processing technique that allows the image to be divided into regions with similar properties such as gray levels, textures, brightness, and contrast. In the case of medical images, the segmentation in cardiac images varies depending on the specific application on the internal structure to be evaluated from the echocardiogram. However, factors such as noise, low resolution, artifacts, or movement may be found in the image that distort the image [11].

One of the most used methods for this type of image is the threshold technique where the gray level (g) is compared in two segments (0 and 1) where the 0 is the darkest and gray level 1 is the lightest as Equation 1.

$$\text{Tglobal}(g) = \begin{cases} 0 & \text{if } g < t \\ 1 & \text{if } g > t \end{cases} \quad (1)$$

To analyze and process any image we should know that an image is generated from a set of pixels denoted as N; for each image level there are a set of pixels denoted as n1. Gray level histogram is normalized and regarded as a probability distribution. (L-1 is the lightest)

$$\sum_{i=0}^{L-1} iPi \quad Pi = ni/N \quad (2)$$

The total mean of the image can be represented as:

$$\mu T = \sum_{i=0}^{L-1} iPi \quad (3)$$

3.2 Convolutional Neuronal Networks

Convolutional Neural Networks (CNN) as shown in Figure1. is a Deep Learning algorithm which can take in an input image, assign importance (learned weights and biases) to various aspects in the image and be able to differentiate one from the other. These types of networks are based on a mathematical operation called convolution, since they carry out the convolution of the input signal layer with respect to a transfer function found at the output of the neuron. These layers perform operations that alter the data in order to learn specific characteristics of that data. The 3 most frequent layers are the convolution which subjects the input images to a set of convolutional filters, each of which activates certain characteristics of the images, an activation that is the Rectified Linear Unit (ReLU), this allows to assign the negative values to zero and keep the positive values, since only the activated characteristics go to the next layer and the Pooling layer that helps to simplify the output by decreasing the non-

linear sample rate, reducing the number of parameters that the network needs to learn [12].
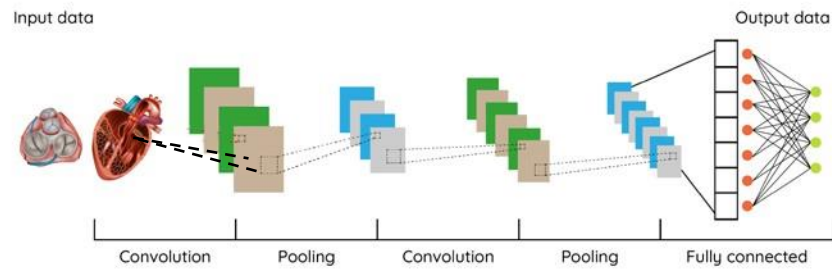

Figure 1. Convolutional Neural Network

3.3 Whale Optimization Algorithm

The Whale Optimization Algorithm (WOA) as show in Figure 2. Is a meta-heuristic optimization algorithm and was proposed by Mirhalili and Lewis in 2016 [13]
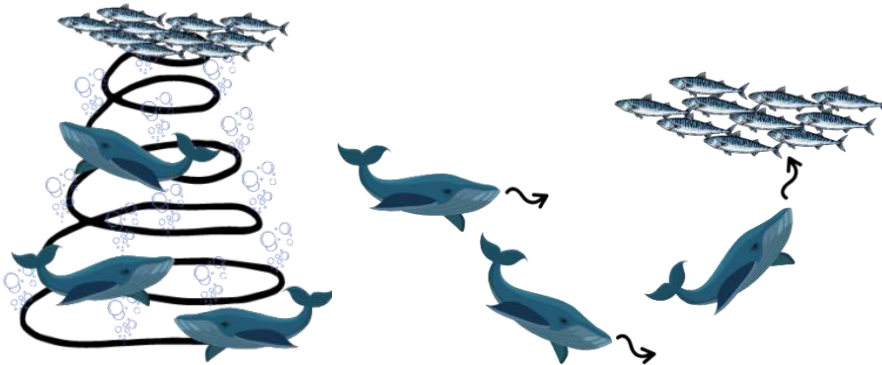

Figure 2. Hunting prays process of Whales in Bubble Nets.

It is inspired by the strategy of hunting prey in the form of Bubble Nets, and there are two maneuvers associated with feeding the bubble network are the upward spirals where the whales dive about 12 meters down and then begin to create spiral-shaped bubbles around the prey and swim to the surface and double loops that include three different stages [14].

3.3.1. Encircling prey

In first stage the search agent (whale) looks for the best solution (the prey) randomly based on the position of each agent. We update the position of a search agent during this phase by using a randomly selected search agent rather than the best search agent. The equation is the following:

$$\vec{D} = \left| \vec{C}.\vec{X}best(t) - \vec{X}(t) \right| \quad (4)$$

$$\vec{X}(t+1) = \vec{X}best(t) - \vec{A}\vec{D} \quad (5)$$

Where:
$\vec{D}$ is the distance vector
$\vec{A}$ and $\vec{C}$ are coefficient vectors
$\vec{X}best$ is the position vector of the best solution
 t indicates the current iteration

The coefficients $\vec{A}$ and $\vec{C}$ represent the iteration for search the prey, in the above formula, rand is a random number between [0, 1], is a control parameter, and it decreases linearly from 2 to 0 with increasing of the iterations. The expression is as follows:

$$\vec{A} = 2a.rand - a \quad (6)$$
$$\vec{C} = 2.rand \quad (7)$$

3.3.3. Bubble-Net Attacking Model

In this phase of exploitation, the bubble network is used to attack the prey. Spiral updating position: This approach first calculates the distance between the whale located at (X, Y) and prey located at (X', Y') as shown in Figure 3. A spiral equation is then created between the position of whale and prey to mimic the helix-shaped movement of humpback whales as follows:

$$\vec{X}(t+1) = \vec{D}.e^{bl}.\cos(2\pi l) + \vec{X}best(t) \quad (8)$$

Where $\vec{D} = \left| \vec{C}.\vec{X}best(t) - \vec{X}(t) \right|$ and indicates the distance of the iteration whale to the prey (best solution obtained so far), b is a constant for defining the shape of the logarithmic spiral, l is a random number in $[-1,1]$.
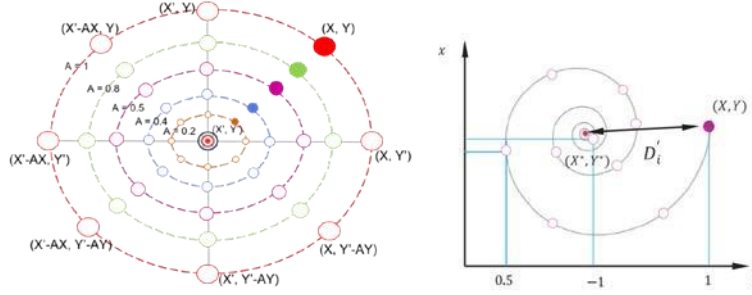
Figure 3. Exploration mechanism implemented in WOA (a) X is randomly chosen search agent, (b) the encircling mechanism and spiral updating position.

3.3.2. Search for prey

If |A|>1, randomly select the whale to replace the current optimal solution; it can keep the whale away from the current reference target and enhance the algorithm's global exploration capabilities and also need to find a better prey to replace the current reference whale. The mathematical model is:

$$C = |\vec{C}.\vec{X}rand(t) - \vec{X}(t)| \qquad (9)$$
$$\vec{X}(t + 1) = \vec{X}rand(t) - \vec{A}\vec{D} \qquad (10)$$

Where $\vec{X}rand$ means randomly selecting the new position vector of the whale.

3.3.3. WOA algorithm

Step 1: Initialize the whale's population $X = (i = 1,2, ...n)$
Step 2: Calculates fitness of each search agent $\vec{X}best$
Step 3: while (t < maximum number of iterations)
　　　　For each agent update a, $\vec{A}$, $\vec{C}$, l and p
　　　if ($|\vec{A}| < 1$)
　　　　Update agent in equation (4)
　　　Else:
　　　　Select a random agent $\vec{X}rand$
　　　　Update current agent by equation (10)

　　　　end-for
　　　　　Check if any search agent goes beyond the search space and amend it
　　　　　Calculate fitness of each search agent
　　　　Update $\vec{X}best$ if there is a better solution
　　　t=t+1
　　　end-while
Step 4: return $\vec{X}best$

4. Data Set and Analysis

For this work, 20 echocardiographic images of the view of the Aortic Valve with Stenosis with a maximum size of 125 x 125 pixels were used, obtained from the free database page: https://openi.nlm.nih.gov /. It was analyzed under medical supervision that the database was indeed of Severe Aortic Stenosis to determine the region that needs to be highlighted with the segmentation and images with noises or echocardiographic views that did not comply with this parameter were discarded.

5. Proposed Model

As shown in figure 4, to initialize the echocardiogram database is loaded into the Matlab interpreter program, using Live Script and the Deep Learning Toolbox. To initialize the segmentation process, the images have a maximum resolution of 125x125 pixels when going through the first cycle, so we start by applying a medfilt2 media filter. To test the WOA algorithm with echocardiographic images, the threshold technique will be used, which consists of a pixel-by-pixel comparison determining the threshold and it is necessary to analyze the region of interest to be isolated in order to find a characteristic gray level. With the global method of the threshold value, the optimum is chosen for each image, it is very sensitive to variations in the brightness of the image, however, it serves very well to separate background objects in the image, such as echocardiograms, the technique is simple, the lowest value is chosen as the threshold. Then the CNN compare the database against a manually segmented echocardiogram of Severe aortic Stenosis valve equally supervised with the specialist.
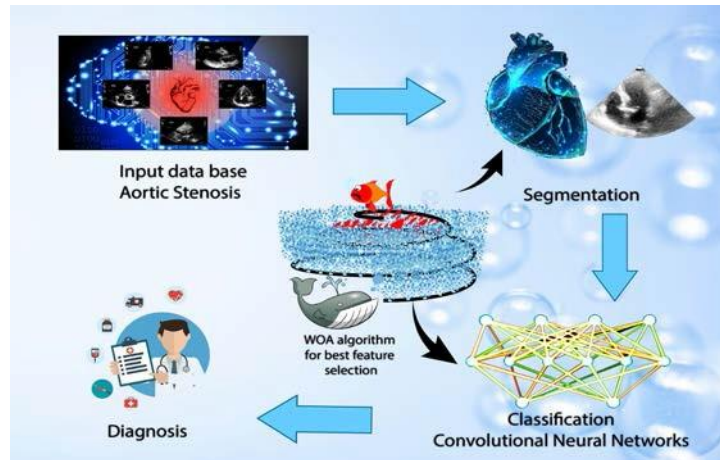

Figure 4. Proposed model Detection of Stenosis Aortic using WOA
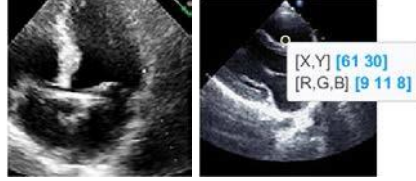
6. Results

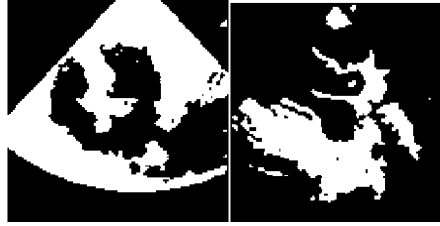Figure 5. Input Dataset of Stenosis Aortic Echocardiogram.

Figure 6. Image preprocessing output segmentation

Comparison of performance in echocardiographic images Figure 5 shows the original images and Figure 6 shows the performance of image preprocessing as a result of a fast fitness function convergence. The Table 1. Presents MSE, PNSR and SSIM of the sample images. With the help of these parameters, the efficiencies of the algorithm are evaluated.

MSE (Mean Square Error) - It is the cumulative square error between the segmented image and the original, the equation used is as follows:

$$MSE = \frac{1}{MN} \sum_{i=1}^{M} \sum_{i=1}^{N} [I(i,j) - I'(i,j)] \quad (10)$$

The PSNR (Peak Signal to Noise Ratio) is the relationship between the peak signal and the noise signal that is introduced by segmentation. It is usually measured in dB and a high PSNR value indicates better reconstruction, the equation is as follows:

$$PSNR = 10log10 \left(\frac{255^2}{MSE} \right) \quad (11)$$

The Structural Similarity Index (SSIM) measures the similarity between two images the equation is as follows:

$$SSIM(x,y) = \frac{(2\mu_X\mu_Y + C1)(2\sigma_{XY} + C2)}{(\mu^2{}_X + \mu^2{}_Y + C1)(\sigma^2{}_X + \sigma^2{}_Y + C2)} \quad (12)$$

Image	T Global (g)	MSE	PSNR	SSIM
AO1	0.341176470588235	204.9158	25.0490	0.9682
AO2	0.396078431372549	161.1288	26.0931	0.9678
AO3	0.286274509803922	144.2471	26.5737	0.96432
AO4	0.290196078431373	92.0355	28.5252	0.8954
AO5	0.266666666666667	138.3398	26.7556	0.9634
AO6	0.360784313725490	89.9684	28.6239	0.9888
AO7	0.321568627450980	159.6673	26.1326	0.9678
AO8	0.309803921568627	184.5939	25.5105	0.9694
AO9	0.482352941176471	246.7908	24.2415	0.9756
AO10	0.337254901960784	195.8529	25.2455	0.9634
AO11	0.431372549019608	199.3229	25.2455	0.9682
AO12	0.462745098039216	228.8476	24.5996	0.96432
AO13	0.333333333333333	121.5998	27.5078	0.9854
AO14	0.396078431372549	131.1748	26.9863	0.9854
AO15	0.360431372549067	89.9684	28.6239	0.9743
AO16	0.360784313725490	207.827	24.9878	0.9523
AO17	0.266666666666667	62.2687	30.2221	0.9877
AO18	0.454901960784314	223.3310	24.5514	0.96432
AO19	0.360784313725490	89.9684	28.6239	0.9567
AO20	0.376470588235294	230.6970	24.5344	0.9634

Table 1. WOA Parameter results.

6.1 Neuronal Network Result

The configuration of the neural network as input the images are 125 x125 pixels, a total of 15626 neurons with 25 convolutional filters size 5 and 2 by 2 max pooling, the padding is used so that the resulting image has the same size as the input and to activation is used by RELU.

An epoch refers to a cycle through the complete training data set, it is once all the images are processed once individually or back and forth, in this case we evaluate in 4 epochs, the loss is calculated in the training and validation and your interpretation is how well the model is doing for these two sets. Unlike precision, it is a sum of the errors made for each example in the training or validation sets for this training of 30 iterations, so the precision of the model is 78%.
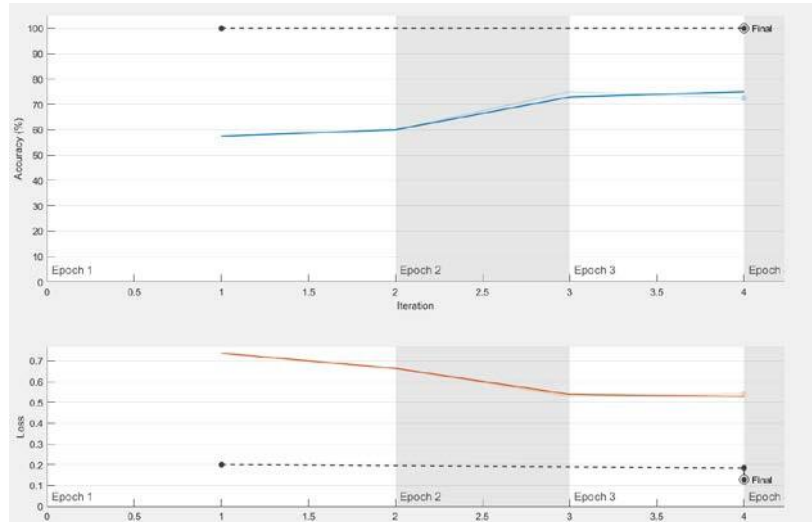
Graphic 1. Accuracy and Loss from Convolutional Neural Network

7. Conclusions

A WOA whale search optimization technique has been proposed to find the global optimal threshold in severe aortic stenosis segmentation images and the results demonstrate that WOA can be used effectively, and convergence is fast. The input performance is compared to the input and output images and shows the effectiveness of the proposed design on the existing segmentation. As for CNN, a larger database is recommended to obtain better accuracy parameters.

7.1 Future Research

Echocardiographic image segmentation, convolutional neural networks, and the whale optimization algorithm (WOA) are novel fields of research to explore and implement reliable, robust, and accurate algorithms. The study can be extended to compare it with other new algorithms to improve performance such as metaheuristic algorithms associated with bubble models of cetaceans (blue whales) and their variants such as Location of prey for tracking the navigation of the Whale Shark, Echolocation based on Herd -Beluga Whale and Segmentation. of Multipoint Monitoring as "Vaquita Marina". Likewise, through an Environmental Intelligence System (AmI) it is proposed to use a Medical Blackboard that allows the use of Echocardiograms to determine if a congenital disease is associated with a variety of symptoms and a comparison with specialists in other parts of the world. Finally, and very important, future work is intended to use a large database obtained from a medical center in Mexico with its proper bioethics formats, to obtain more parameters that can determine the degree of damage or prediction of aortic stenosis with the help of the specialist

References

[1] Fonseca MYI, Díaz RYL, Vargas FMÁ. Relación entre la COVID-19 y las enfermedades cardiovasculares. 16 de abril. 2020;59(277):1-6.

[2] Martínez, A. D., Ochoa, A., & Rodríguez, J. R. (2019). A Hybrid Intelligent System for Improving a Health Model Associated with Cardiovascular Disease. Res. Comput. Sci., 148(6), 13-23.

[3] Carità, P., Coppola, G., Novo, G., Caccamo, G., Guglielmo, M., Balasus, F., Novo, S., Castrovinci, S., Moscarelli, M., Fattouch, K., & Corrado, E. (2016). Aortic stenosis: insights on pathogenesis and clinical implications. Journal of geriatric cardiology: JGC, 13(6), 489–498.

[4] Ochoa, A., Hernández, A., Cruz, L., Ponce, J., Montes, F., Li, L., & Janacek, L. (2010). Artificial societies and social simulation using ant colony, particle swarm optimization and cultural algorithms. In *New Achievements in Evolutionary Computation*. IntechOpen.

[5] Abd El Aziz, M., Ewees, A. A., & Hassanien, A. E. (2017). Whale optimization algorithm and moth-flame optimization for multilevel thresholding image segmentation. Expert Systems with Applications, 83, 242-256.

[6] Nasiri, J., & Khiyabani, F. M. (2018). A whale optimization algorithm (WOA) approach for clustering. Cogent Mathematics & Statistics, 5(1), 1483565.

[7] Vijh, S., Gaur, D., & Kumar, S. (2020). An intelligent lung tumor diagnosis system using whale optimization algorithm and support vector machine. International Journal of System Assurance Engineering and Management, 11(2), 374-384.

[8] Fang, H., Fan, H., Lin, S., Qing, Z., & Sheykhahmad, F. R. (2021). Automatic breast cancer detection based on optimized neural network using whale optimization algorithm. International Journal of Imaging Systems and Technology, 31(1), 425-438.

[9] Tongbram, S., Shimray, B. A., Singh, L. S., & Dhanachandra, N. (2021). A novel image segmentation approach using fcm and whale optimization algorithm. Journal of Ambient Intelligence and Humanized Computing, 1-15.

[10] Oliva, D., Abd El Aziz, M., & Hassanien, A. E. (2017). Parameter estimation of photovoltaic cells using an improved chaotic whale optimization algorithm. Applied energy, 200, 141-154.

[11] Gonzalez, Rafael C., and Richard E. Woods. "Digital image processing." (2002).

[12] Haykin S. (2009), Neural Networks and Learning Machines (3rd Edition), Prentice Hall.

[13] S. Mirjalili and A. Lewis, "The whale optimization algorithm," Advances in Engineering Software, vol. 95, pp. 51–67, 2016.

[14] M. H. Zhong and W. Long, "Whale optimization algorithm based on stochastic adjustment control parameter," Science Technology and Engineering, vol. 17, no. 12, pp. 68–73, 2017.